

**STUDY ON THE ELECTROCHEMICAL
PERFORMANCE OF CARBON-BASED PLANAR
SUPERCAPACITOR IN AQUEOUS ELECTROLYTE**



**A Thesis Submitted in Partial Fulfillment of the Requirement for the
Degree of Doctor of Philosophy in Physics
Suranaree University of Technology
Academic Year 2020**

การศึกษาประสิทธิภาพทางไฟฟ้าเคมีของตัวเก็บประจุยิ่งยวดแบบแผ่น
ในสารละลายอิเล็กโทรไลต์ที่มีน้ำเป็นตัวทำละลาย

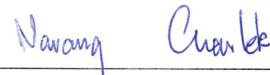


วิทยานิพนธ์นี้เป็นส่วนหนึ่งของการศึกษาตามหลักสูตรปริญญาวิทยาศาสตรดุษฎีบัณฑิต
สาขาวิชาฟิสิกส์
มหาวิทยาลัยเทคโนโลยีสุรนารี
ปีการศึกษา 2563

**STUDY ON THE ELECTROCHEMICAL PERFORMANCE OF
CARBON-BASED PLANAR SUPERCAPACITOR IN AQUEOUS
ELECTROLYTE**

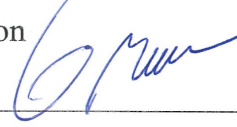
Suranaree University of Technology has approved this thesis submitted in partial fulfillment of the requirements for Degree of Doctor of Philosophy.

Thesis Examining Committee



(Dr. Narong Chanlek)

Chairperson



(Assoc. Prof. Dr. Worawat Meevasana)

Member (Thesis Advisor)



(Assoc. Prof. Dr. Sirichok Jungthawan)

Member



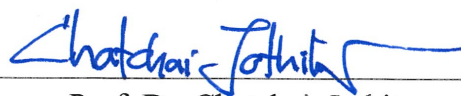
(Asst. Prof. Dr. Wittawat Saenrang)

Member



(Dr. Ittipon Fongkaew)

Member



(Assoc. Prof. Dr. Chatchai Jothityangkoon)

Vice Rector for Academic Affairs
and Quality Assurance



(Prof. Dr. Santi Mansiri)

Dean of Institute of Science

อุกฤษฏ์ จิตโรภาส : การศึกษาประสิทธิภาพทางไฟฟ้าเคมีของตัวเก็บประจุยิ่งยวดแบบแผ่น
ในสารละลายอิเล็กโทรไลต์ที่มีน้ำเป็นตัวทำละลาย (STUDY ON THE
ELECTROCHEMICAL PERFORMANCE OF CARBON-BASED PLANAR
SUPERCAPACITOR IN AQUEOUS ELECTROLYTE). อาจารย์ที่ปรึกษา :
รองศาสตราจารย์ ดร.วรวัดน์ มีวาสนา, 64 หน้า

ลักษณะเด่นที่สำคัญของอุปกรณ์กักเก็บพลังงานแบบตัวเก็บประจุยิ่งยวด คือความสามารถ
ในการอัดและคายประจุอย่างรวดเร็ว นอกจากนี้ยังมีอายุการใช้งานที่ยาวนานกว่าแบตเตอรี่ทั่วไป
หลายเท่าตัว แต่การเพิ่มอัตราการอัดประจุให้เร็วมากขึ้นนั้น จะส่งผลทำให้ค่าความจุไฟฟ้าโดยรวม
ลดลง ซึ่งส่งผลเสียต่อการทำหน้าที่เป็นแหล่งกักเก็บพลังงานที่ดี เพื่อหลีกเลี่ยงปัญหาดังกล่าว ตัว
เก็บประจุยิ่งยวดที่มีอิเล็กโทรดแบบแผ่นจึงถูกนำมาประยุกต์ใช้ เนื่องจากอิเล็กโทรดแบบแผ่นนี้จะ
สามารถช่วยในการเคลื่อนที่ของประจุและเพิ่มความสามารถของการอัดประจุในอัตราที่สูงได้ ใน
งานวิจัยนี้ เป็นการศึกษาและตรวจสอบค่าความจุไฟฟ้าจำเพาะของตัวเก็บประจุยิ่งยวดที่ใช้คาร์บอน
เป็นวัสดุทำปฏิกิริยาและจัดวางอิเล็กโทรดเป็นแบบแผ่น แถบของขั้วไฟฟ้าที่มีลักษณะต่าง ๆ ถูก
พิมพ์ลงบนแผ่นวงจรพิมพ์และนำไปใช้กับสารละลายอิเล็กโทรไลต์ที่มีน้ำเป็นตัวทำละลาย ไชคลิก
โวลแทมเมตรีแบบสองขั้วเป็นเทคนิคที่ถูกนำมาใช้ตรวจสอบความสามารถในการอัดและคายประจุ
ของอุปกรณ์ตัวอย่างที่ออกแบบขึ้น ในการวิเคราะห์ผลการทดลอง ค่าความจุไฟฟ้าอันเนื่องมาจาก
แรงทางไฟฟ้าและค่าความจุไฟฟ้าอันเนื่องมาจากปฏิกิริยาเคมีถูกทำให้แยกออกจากกัน ได้ชัดเจน
โดยใช้การซ้อนทับของรูปโครงสร้างจากการวัด ไชคลิก โวลแทมเมตรีในสารละลายที่มีความเข้มข้น
ต่างกัน จากการทดสอบพบว่าค่าความจุไฟฟ้าของตัวเก็บประจุยิ่งยวดแบบแผ่นมีค่าเพิ่มสูงขึ้นตาม
การอัดประจุด้วยอัตราที่สูงขึ้น โดยมีค่าความจุไฟฟ้าจำเพาะที่มากกว่าค่าเริ่มต้น แม้อัตราการอัด
ประจุจะเพิ่มขึ้นเป็นหนึ่งร้อยเท่า ซึ่งแตกต่างจากตัวเก็บประจุยิ่งยวดทั่วไป ความสามารถในการอัด
ประจุในอัตราที่สูงโดยไม่สูญเสียความจุโดยรวมนี้ ทำให้ตัวเก็บประจุยิ่งยวดแบบแผ่นมี
ประสิทธิภาพที่ดีกว่าตัวเก็บประจุยิ่งยวดทั่วไป

สาขาวิชาฟิสิกส์
ปีการศึกษา 2563

ลายมือชื่อนักศึกษา _____
ลายมือชื่ออาจารย์ที่ปรึกษา _____

UKRIT JITROPAS : STUDY ON THE ELECTROCHEMICAL
PERFORMANCE OF CARBON-BASED PLANAR SUPERCAPACITOR IN
AQUEOUS ELECTROLYTE. THESIS ADVISOR : ASSOC. PROF.
WORAWAT MEEVASANA, Ph.D. 64 PP.

ENERGY STORAGE DEVICE/SUPERCAPACITOR/PLANAR ELECTRODE

Besides offering a very long life cycle, one of the significant characteristic of supercapacitor is to be able to rapidly charge-discharge much faster than the battery. The increase of charging rate unfortunately results in capacitance reduction which is not preferable for energy storage device. To avoid the conflict, planar interdigitated electrode which facilitates ions mobility and provides good rate capability is usually implemented. Here, the specific capacitance of carbon based planar comb-like electrodes were investigated. The current collectors of varied electrode width were patterned on printed circuit board. Two electrode system of cyclic-voltammetry (CV) technique were conducted using aqueous electrolyte. Electric double layer and redox contribution on the total capacitance were distinguish by mapping CV profile obtained from difference electrolyte concentration. The capacitance of all planar samples interestingly increases to the maximum peak and remains higher than its initial value even at 100 times increasing of scan rate. This excellent rate capability observed here indicates the superior electrochemical performance of planar electrode configuration beyond the conventional sandwich structure.

School of Physics

Academic Year 2020

Student's Signature

Advisor's Signature



ACKNOWLEDGMENTS

My thesis would not have been possible without the support of many people. Firstly, I would like to express my gratitude to my thesis advisor, Assoc. Prof. Dr. Worawat Meevasana who invited me to join his research group. I met him for the first time when I was a high school student. At that time, he was an instructor for the Physics Olympiad camp at Suranaree University of Technology. I, as one of his student, watched him analyzed the complex problems by using only simplified physics concepts but he can fluently explain them in the explicit way that I had never seen before. That was the great first impression toward him and made me more interested in physics world. Many years passed, I'm very appreciated and honored to finish my doctoral degree under his supervision. Thank you for all supports and guidance both in academic and real life.

I would like to acknowledge my thesis defense committee members, Dr. Narong Chanlek (Chair person), Assoc. Prof. Dr. Sirichok Jungthawan, Asst. Prof. Dr. Wittawat Saenrang and Dr. Ittipon Fongkaew who offer their valuable time to provide many useful comments and suggestions.

I also would like to thank all members in Meevasana group who support me and provide a very friendly study environment. Especially thank to Mr. Worasarit Saengsui and Mr. Puttimate Thongtan who always provides a good discussion during the experimental and result analysis period.

I am very gratitude for the School of Physics, Institute of Science, Suranaree University of technology to be the good memorable place in my academic life since

high school until the Ph.D. Suranaree University of Technology and the Research Network NANOTEC (RNN) program of the National Nanotechnology Center (NANOTEC), NSTDA, Ministry of Science and Technology, Thailand and the Thailand Research Fund through the Royal Golden Jubilee Ph.D. program (grant number PHD/0099/2560) are acknowledged for the financial support.

I would like to express my truly praise to my father who dedicates all his life supporting his son. He taught me everything. Since I was young, he left the seed and paved the way of logical thinking in every topics we were discussing in daily life. Therefore I grow up to be the man with solid mindset. He graduated his Bachelor's Degree in Physics and I'm very proud to be in the exact same field. Although he passed away many years before I can finish my Doctoral Degree and do not be able to read all these admired sentences, I still wish he would know that his son do his best and I hope that I'm doing him proud. Words cannot explain how I feel, how much I miss him and how much I want to share this moment with him. I also would like to thank to my family and friends who always be by my side providing cares and supports in every steps of my life. Lastly, I would like to thank to myself to be patient throughout all these tough years. Remember that when looking to this thesis book, lots of memories here and you did a great job.

Ukrit Jitropas

CONTENTS

| | Page |
|--|-------------|
| ABSTRACT IN THAI | I |
| ABSTRACT IN ENGLISH | II |
| ACKNOWLEDGMENTS | III |
| CONTENTS | V |
| LIST OF FIGURES | VIII |
| LIST OF TABLES | XII |
| CHAPTER | |
| I INTRODUCTION | 1 |
| 1.1 Background and motivation | 1 |
| 1.2 Objectives of research | 2 |
| 1.3 Scope and limitations | 3 |
| 1.4 Outline of thesis | 3 |
| II LITERATURE REVIEWS & THEORETICAL ASPECTS | 5 |
| 2.1 Literature reviews | 5 |
| 2.1.1 Concept of energy decentralization | 5 |
| 2.1.2 Typical energy storage device | 6 |
| 2.1.3 Experimental on planar electrode supercapacitor | 11 |
| 2.2 Theoretical aspects | 17 |

CONTENTS (Continued)

| | Page |
|--|-------------|
| 2.2.1 Simulation of electric field intensity produced by planar electrode structure | 17 |
| 2.2.2 Dependence of electrode geometry on the cell resistance (K-cell)..... | 19 |
| 2.2.3 Cyclic voltammetry measurement and capacitance calculation..... | 21 |
| 2.2.4 Galvanostatic charge/discharge measurement and capacitance calculation | 23 |
| 2.2.5 Electrochemical Impedance Spectroscopy | 24 |
| 2.2.6 Differentiation of the contribution between EDLC, redox reaction and intercalation pseudocapacitance..... | 25 |
| III METHODS..... | 30 |
| 3.1 Electrode fabrication | 30 |
| 3.1.1 Current collector design and fabrication | 30 |
| 3.1.2 Active material and electrolyte preparation | 32 |
| 3.1.3 Coating process and cell assembly | 33 |
| 3.2 Electrochemical measurement..... | 34 |
| 3.3 Electric field simulation | 35 |
| IV RESULTS AND DISCUSSION..... | 39 |
| 4.1 Specific capacitance and rate capability profile | 39 |
| 4.1.1 Specific capacitance of planar and conventional sandwich structure with respect to scan rate..... | 39 |

CONTENTS (Continued)

| | Page |
|---|-------------|
| 4.1.2 Potential gradient and average electric field intensity simulation results | 43 |
| 4.2 Differentiation between EDLC and redox reaction contribution on the total capacitance..... | 45 |
| 4.2.1 Specific capacitance of planar electrode using varied electrolyte concentration..... | 45 |
| 4.2.2 CV profile mapping technique | 46 |
| 4.2.3 Further discussion on the influence of electrode geometry on the cell capacitance | 55 |
| V CONCLUSIONS..... | 57 |
| 5.1 Conclusions | 57 |
| 5.2 Future direction | 58 |
| REFERENCES | 59 |
| CURRICULUM VITAE..... | 64 |

LIST OF FIGURES

| Figure | Page |
|--|------|
| 2.1 Schematic of conventional parallel plates capacitor | 7 |
| 2.2 Schematic of electrical double layer charge storage at the interface of electrode/electrolyte | 9 |
| 2.3 Ragone plot showing the specific energy and specific power of typical energy storage devices..... | 10 |
| 2.4 Relative capacitance for micro-devices made of 4, 8 and 16 interdigital electrodes..... | 12 |
| 2.5 The design of in-plane electrode with a) 2 sub-electrodes I-Ps(2), b) 4 sub-electrodes I-Ps(4), c) 6 sub-electrodes, d) conventional sandwich structure and e) cell assembly | 14 |
| 2.6 a) Volumatic stack capacitance of planar and sandwich sample and b) Nyquist plot of each sample | 14 |
| 2.7 Images of micro supercapacitor(MCS) a) MSCs32, b) MSCs16, c) MSCs8 and optical image of electrode fringe (d-f)..... | 16 |
| 2.8 Stack capacitance of each micro and sandwich supercapacitor | 16 |
| 2.9 Electric field of (a) sandwich and (b) planar supercapacitor..... | 18 |
| 2.10 2-D cross section simulation of electric field intensity along the electrode and interspace | 18 |

LIST OF FIGURES (Continued)

| Figure | Page |
|---|-------------|
| 2.11 2-D cross section simulation of potential distribution..... | 19 |
| 2.12 Illustration of interdigitated electrode dimension..... | 20 |
| 2.13 Comparison of cell constant value obtained between Olthuis <i>et al.</i> work and simplified approximation model..... | 21 |
| 2.14 Typical voltammetry characteristic and respective equivalent circuit of a) an ideal EDLC, b) EDLC with series resistance, c) real EDLC and d) pseudocapacitor | 22 |
| 2.15 Voltage-time profile obtained from GCD measurement | 24 |
| 2.16 Nyquist plot of the respective equivalent circuit of a) an ideal EDLC, b) EDLC with series resistance, c) EDLC with series and parallel resistance and d) Randle circuit with Warburg impedance..... | 25 |
| 2.17 The b-value with respect with scan rate of Mxene multilayer material | 28 |
| 2.18 The CV profile at a) 20mV/s, b) 2mV/s and the contribution of surface and bulk process on the total capacitance..... | 29 |
| 3.1 Schematic of planar electrode of a) Type2 (2mm.), b) Type3 (3mm.), c) Type4 (4 mm.) fringe width and d) sandwich structure | 31 |
| 3.2 Active material preparation process of a) pre-mixed binder, b) Carbon ink and c) ball mill..... | 32 |
| 3.3 Schematic of printed circuit board cover with remove sticker mask for coating process..... | 33 |

LIST OF FIGURES (Continued)

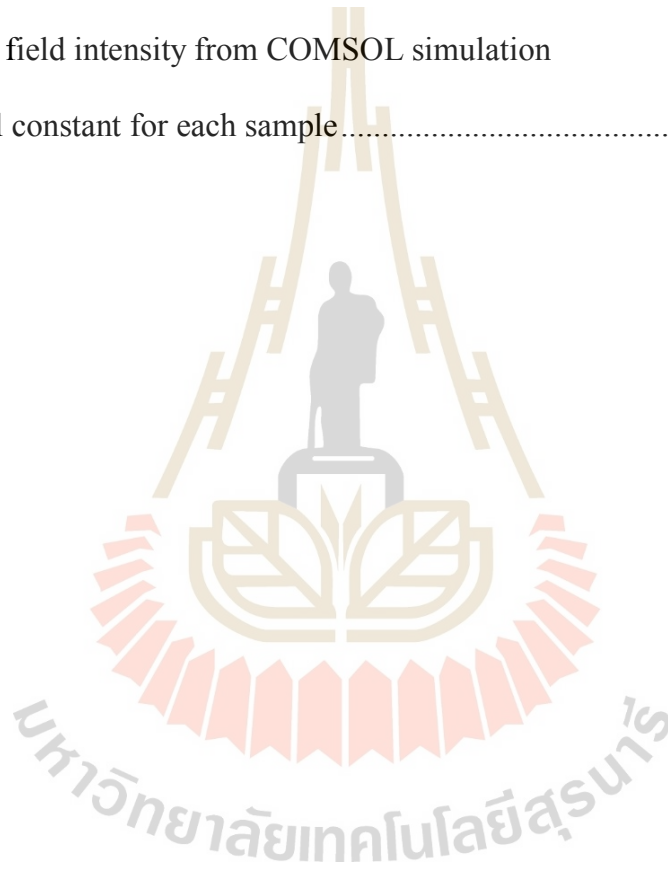
| Figure | Page |
|--|-------------|
| 3.4 Coating process a) electrode, b) doctor blade coating and c) drying process | 33 |
| 3.5 Planar electrode supercapacitor with array ratio of a) 2:1, b) 3:1, c) 4:1 and d) real two electrode system set up..... | 34 |
| 3.6 CV profile of type 2 planar electrode at scan rate of 100 mV/s..... | 35 |
| 3.7 COMSOL simulation a) electrode geometry, b) ground boundary, c) terminal boundary and d) meshing of the model domain..... | 36 |
| 3.8 COMSOL simulation a) potential gradient, b) electric field intensity of the planar electrode..... | 38 |
| 4.1 a) Specific capacitance with respect to scan rate of each sample and b) Relative capacitance with respect to scan rate of each sample | 40 |
| 4.2 GCD profile with varying discharging current..... | 41 |
| 4.3 Relative capacitance with respect to discharging current obtained From galvanostatic charge/discharge measurement..... | 42 |
| 4.4 Potential gradient of planar electrode with a) 2mm, b) 3mm and c) 4mm fringe width. Electric field line of d) planar and e) sandwich structure..... | 43 |
| 4.5 Capacitance with respect to scan rate of planar electrode in 2M and 4M sodium sulfate electrolyte..... | 45 |
| 4.6 CV profile of planar electrode in 2M and 4M sodium sulfate electrolyte at scan rate of a) 2 mVs ⁻¹ , b) 20 mVs ⁻¹ , c) 80 mVs ⁻¹ and 200 mVs ⁻¹ | 47 |

LIST OF FIGURES (Continued)

| Figure | Page |
|---|------|
| 4.7 Nyquist plot of the cell using carbon-based electrode and sodium nitrate electrolyte | 48 |
| 4.8 Plot of $\log(i)$ and $\log(v)$ used in b-valued determining | 49 |
| 4.9 Contribution of EDLC and redox reaction on total specific capacitance of 2M and 4M electrolyte concentration | 50 |
| 4.10 a) EDLC and b) redox contribution on the total capacitance | 52 |
| 4.11 Simplified mathematical model fitting of a) EDLC and b) redox contribution | 54 |
| 4.12 Ratio between redox and EDLC contribution | 55 |

LIST OF TABLES

| Table | Page |
|--|------|
| 4.1 Maximum capacitance from CV measurement and average electric field intensity from COMSOL simulation and cell constant for each sample..... | 44 |



CHAPTER I

INTRODUCTION

1.1 Background and motivation

The concern about fossil fuel depletion in recent decades promotes the rise of many alternative renewable energy sources such as solar, thermal, hydropower and wind energy. These unlimited resources can be converted to the useful electrical energy supplying to the household, industrial and transportation demand. Unfortunately, there is a restriction of the operation condition for these energy sources such as day-time (solar energy) and suitable location (thermal, hydropower and wind energy). The need of compact electrical energy storage device therefore becomes an intense issue. Besides the conventional battery, supercapacitor which can deliver a very high power and has almost unlimited life cycle is an outstanding energy storage device in the present day.

Supercapacitor or Electric Double Layer Capacitor (EDLC) stores electrical charge using electrostatic force between electrode and electrolyte ions. Similar to a conventional capacitor, the capacitance of the device depends on the area of the electrode. Activated carbon and other carbon based materials is frequently used as the active material for electrode due to its vary large surface area. Metal oxide and conducting polymer, which provide an extra redox pseudo-capacitance, are also normally added in the electrode in order to increase the total capacitance. In addition to

active material, electrode configuration plays a crucial role to the electric field between electrodes and therefore effects the storage capacity of the device.

Conventional supercapacitor has a sandwich structure which positive and negative electrode are in opposite side. The separator is inserted in between to prevent a short circuit problem. Unlike this sandwich structure, supercapacitor with planar electrode, which positive and negative are in the same plane, provides an alternative electrode configuration. Electrodes are placed in the base leaving the gap space between them. The separator therefore do not need in this case. Electrode of planar supercapacitor can be designed in many patterns. In this work, we would like to investigate the influence of electrode geometry on the charging characteristic and specific capacitance of the planar supercapacitor. The final outcome will then be used to optimize the charging condition which provides highest specific capacitance for each electrode pattern.

1.2 Objectives of research

- 1) To investigate the influence of electrode geometry on the specific capacitance of planar supercapacitor
- 2) To differentiate the contribution of electric double layer and redox pseudocapacitance with respect to charging rate
- 3) To provide a general guideline of the optimized charging condition in order to obtain highest capacitance

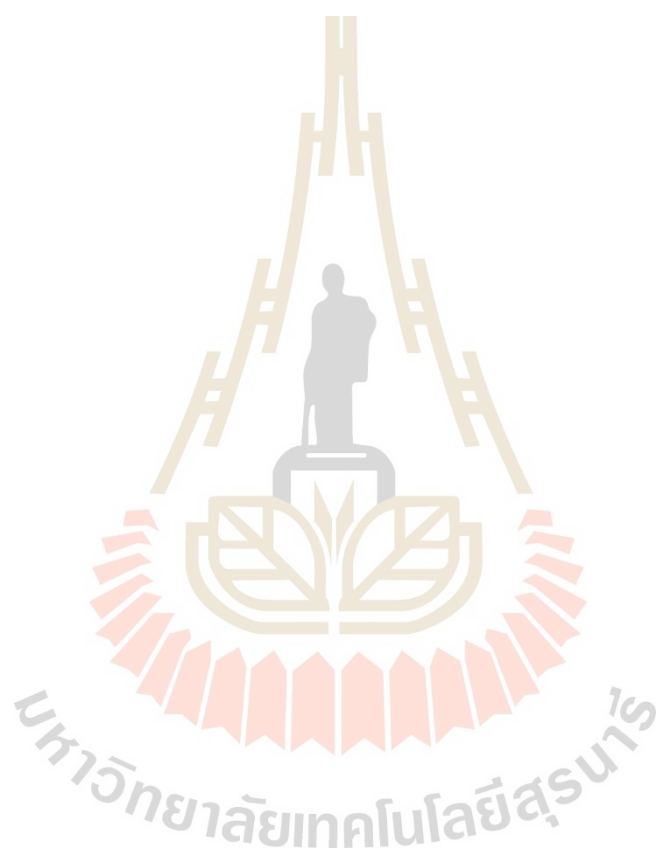
1.3 Scope and limitations

- 1) Comb-like electrode configurations are selected as a periodic planar geometry which facilitates the methodically study.
- 2) Activated carbon, as a common type of carbon-based material used in supercapacitor research area, is implemented as an electrode active material
- 3) In order to acquire the capacitance and the information of charge storage mechanism, electrochemical performance of all samples are mainly investigated using Cyclic Voltammetry (CV) technique

1.4 Outline of thesis

This thesis is arranged in 5 chapters. In chapter I, background and motivation of energy decentralization and the need of electrical energy storage device are proposed. Supercapacitor is preferred as an outstanding energy storage device which its performance meet the industry desire. Chapter II is the literature review which summarizes the previous research works related to energy storage device, especially supercapacitor. Charge storage mechanism of supercapacitor and how to increase its capacitance are explained. Planar electrode configuration, one approach to enhance its performance, is discussed from both experimental and theoretical aspect. Cyclic voltammetry is reviewed as the main technique used to measure and evaluated the electrochemical performance of the device. Chapter III illustrates the experimental methods including the material preparation, electrode fabrication, electrochemical measurement and simulation work. Chapter IV summarizes and discusses the outstanding obtained results. In this chapter, the approach to differentiate the

contribution of EDLC and redox from total capacitance is initiated. The simplified model of charge storage mechanism of the device is proposed. Chapter V is the conclusion of the thesis work including the suggestion future implementation.



CHAPTER II

LITERATURE REVIEWS & THEORETICAL ASPECTS

This chapter is separated into two parts. First, the literature review which indicates the concept of energy decentralization and the need of energy storage devices including battery, conventional capacitor and supercapacitor. Among them, supercapacitor with planar electrode configuration is an outstanding one providing most of the desired characteristic of excellent energy storage device. The experimental research works on planar interdigitated electrode are examine. Second part is the simulation model and theoretical aspect which support and indicated the root causes making the planar electrode more superior than conventional sandwich structure.

2.1 Literature reviews

2.1.1 Concept of energy decentralization

Energy decentralization is said to be an effective concept of future energy supply system for household and industrial unit. This concept aims to put the power source close to the end user regardless of relying on the main distribution network. The concept is further used in transportation section such as an electric vehicle which provide a better efficiency and lower environmental impact (Alanne et al., 2006). Beside the fossil fuel which is in a depletion state and will vanish within decades, there are many alternative renewable energy sources such as wind, solar and hydropower. These energy sources are accessible for everyone, even in the remoted area, and make

the concept of energy decentralization possible. Unfortunately, solar energy is available only in day-time while wind and hydropower are also capable only in the proper location. Electrical energy storage devices are therefore needed in order to keep and ensure the continuous energy supply to every individual unit. Main characteristics of an excellent energy storage device are to be able to store large amount of energy, support fast charging process, deliver high power output and provide a long operation life cycle (Aneke et al., 2016).

2.1.2 Typical energy storage device

Battery is the most common electrical energy storage device used in many areas. It can store a very large amount of energy by means of the chemical-based charge/discharge mechanism. The operation potential window of the battery is relatively high which enlarge its capacity since the amount of energy stored depends on the square of rated voltage. Unavoidably, by employing the chemical reaction, battery do not support the fast charging and can provide only low power output because the charge storage mechanism requires some length of time to complete the chemical reaction process. The operation life of battery is relatively short because the degradation of electrode after many charging and discharging cycles. Since the battery compose of toxic chemical agent, the recycle process require the specific procedure in order to avoid the environmental impact issue.

Without introducing electrochemical reactions, conventional capacitor stores charges using pure electrostatic force across the parallel plate electrode as illustrated in figure 2.1. The operation cycle of capacitor is very large, theoretically infinite, because the charge storage mechanism do not involve with any reaction. Pure electrostatic force

produced by the external voltage across the plates accumulates charge instantly. Capacitor therefore be able to charge within short period and can deliver high power output (Simon et al., 2014). The capacitance is determined by the following equation

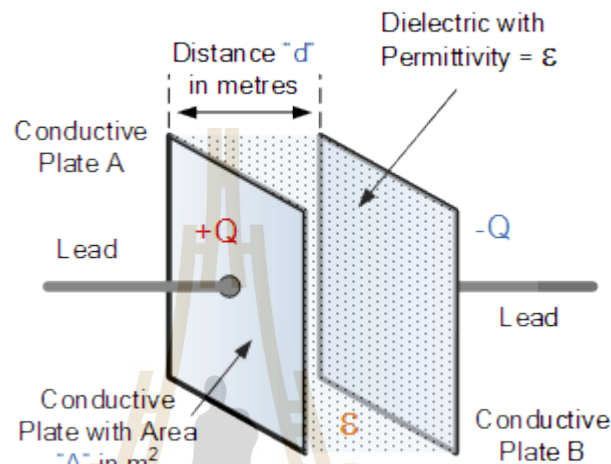


Figure 2.1 Schematic of conventional parallel plate capacitor.

(Source: https://www.electronics-tutorials.ws/capacitor/cap_1.html).

$$C = \epsilon A/d \quad (2.1)$$

Where C is capacitance ϵ is a relative permittivity, A is electrode area and d is the separation distance between the parallel electrode. Methods of increasing the capacitance are to select the suitable dielectric medium or enlarge the conductive plate area. Good dielectric medium should be thin enough to decrease the separation distance and should provide high relative permittivity. Unfortunately, the relative permittivity of a common dielectric material range from 1.2 (paper) to 1000 (Barium titanate). In order to obtain only one farad capacitor, it would require at least thousands square meters of parallel electrode which is not practical for real compact energy storage device (Libich et al., 2018). The capacitor is therefore using together with the battery

as a regulator to deliver and supply the high power in a short period of time.

In recent years, modern research in energy storage field pays an intense attention to develop the Electrochemical Double-Layer Capacitor (EDLC) or supercapacitor. Similar to the conventional capacitor, supercapacitor accumulates charge at the surface of electrode by means of electrostatic force produced by the applied voltage between parallel plates. Electrolyte, instead of dielectric medium, is used to serve as an ions reservoir. The ions permeable separator is insert between the plates to prevent the short circuit from physical contact of the opposite electrode (Jayalakshimi et al., 2008). Electrode of supercapacitor usually has high specific surface area (SSA) material such as activated carbon, carbon nanotube and other carbon-based material which provide many thousands square meter area per unit gram. This SSA material provide a very large value of the term A in equation 2.1 and therefore increase the capacitance of the device (Iro et al., 2016; Chen et al., 2017). Another unique characteristic of EDLC is the dramatic reduction of the separation distance d . As shown in figure 2.2, the separation distance of the electric double layer is approximately equal to the size of solvent electrolyte ions (Kondrat et al., 2012; Kim et al., 2019). The term d is therefore reduced from the order of millimeter, for conventional dielectric medium, down to nanoscale. The huge increase in electrode surface area (A) and significant reduction of separation distance (d), according to the equation 2.1, result in capacitance enhancement in many order of magnitude (hundreds farad per gram) and make supercapacitor more compatible for energy storage device application than the conventional capacitor (Baptista et al., 2019).

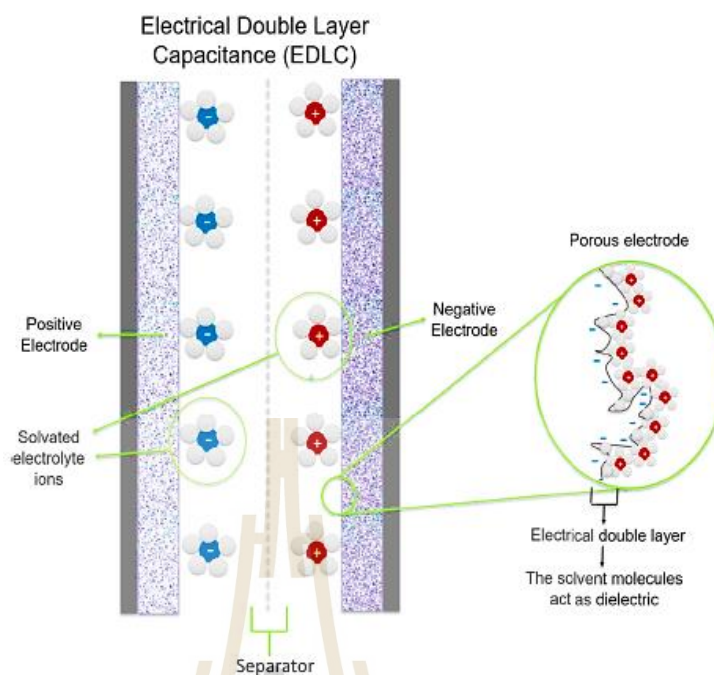


Figure 2.2 Schematic of electrical double layer charge storage at the interface of electrode/electrolyte. (Baptista et al., 2019).

The absence of electrochemical reaction allows supercapacitor to charge/discharge much faster and deliver higher power output than battery. As the Ragone plot illustrated in figure 2.3, supercapacitor characteristic is in between the conventional capacitor and battery. It bridges the gap and combines all desired characteristic of energy storage device such as having relatively large capacity, delivering higher power output and providing very long life cycle. Other advantages of supercapacitor are the ability to efficiently operate for wide range of temperature and generally fabricated by non-toxic material. Further improvement of supercapacitor is therefore aiming to enhance the specific energy toward to the battery. Beside using high SSA carbon-based material which facilitates EDLC, metal oxide and conducting polymer are also implemented as an electrode active material (Simon et al., 2010).

These type of materials provide an additional pseudocapacitance by introducing chemical redox reaction. This charge storage mechanism arises from the chemical interaction between electrode material and electrolyte ions (Abdah et al., 2020). Unlike EDLC which accumulates charge at the interface between electrode and electrolyte, redox-pseudocapacitance store the charge in form of compound ions. The additional capacity consequently depends on the ions available in electrolyte (Zhang et al.,2020; Fan et al., 2006). Unfortunately, the increase in capacitance, by employing some chemical reaction, unavoidably shorten the operation life cycle because of the degradation of electrode and electrolyte.

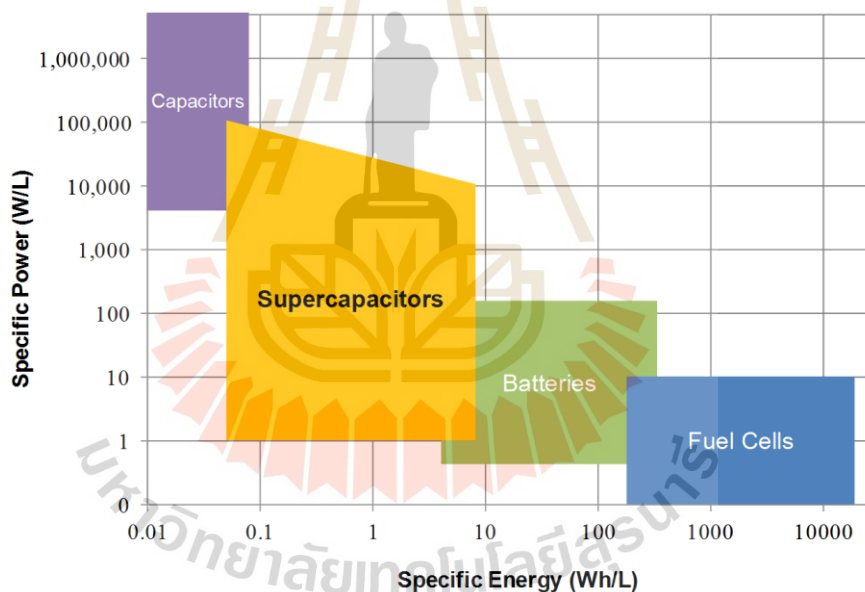


Figure 2.3 Ragone plot showing the specific energy and specific power of typical energy storage devices. (Source: <https://www.cap-xx.com/resource/energy-storage-technologies/>).

Apart from dealing with active material, many researches show that electrode configuration also plays an importance role on the supercapacitor performance. Typical supercapacitor is normally assembled with conventional sandwich structure. The

positive and negative electrodes are parallel placed in opposite side. Separator soaked with electrolyte is insert in between. This electrode layout is scalable for large fabrication. The electric field inside is uniform which facilitate the ions movement. One of the weak points of this assembly is the separator. The compact assembly may cause the damage on the separator. Only small damage can lead to the charge leak and short circuit. The thickness of separator therefore should be thick and dense enough to prevent this issue. Increasing in the thickness of the separator unfortunately also increases the internal resistance and deteriorates performance of the device. Planar interdigitated electrode configuration is an alternative electrode structure in which both positive and negative electrode are place in the same plane leaving the small inter space between them. The separator, in this case, is eliminated and the total internal resistance of the device is decreased. Other advantage of planar structure is an intense electric field at the edges of electrode fringe which help accumulating large amount of ions charge (Ryu et al., 2002; Qi et al., 2017). Experimental and theoretical simulation researches involving electrochemical performance are summarized in the following sections.

2.1.3 Experiment on planar electrode supercapacitor

Besides an appropriate material selection, the geometry of electrode was found to be one of key parameters which determines performance of the device. There are many theoretical determinations and experimental studies indicating the influence of electrode configuration of micro-planar supercapacitor on its specific power and capacitance.

The relative capacitance with respect to the scan rate of micro-planar

supercapacitor for different interdigital electrode patterns are shown in figure 2.4 (Pech et al., 2010). By controlling the same total surface area, electrode length and interspace between electrodes, the relative capacitance of the device was founded to increase with the number of interdigital electrodes (the more number of interdigital electrodes, the narrower electrode width) for the entire scan rate range from 1 to 200 mV/s. The breakthrough of electrochemical performance is mainly caused by the reduction of the mean ionic diffusion path which therefore decrease the electrolyte resistance between electrodes. It is clearly observed that the higher scan rate applied, the lower relative capacitance obtain. This monotonic trend of rate capability appears in both conventional sandwich structure and planar architecture electrode supercapacitor. For a low scan rate, electrolyte ions have much longer time to move toward and reside to the electrode. All accessible surface area of electrode then fully occupy and therefore provide higher capacitance. Among them, micro-planar supercapacitor with larger number of interdigital electrode shows a better rate capability because it has shorter mean ions diffusion path as expected.

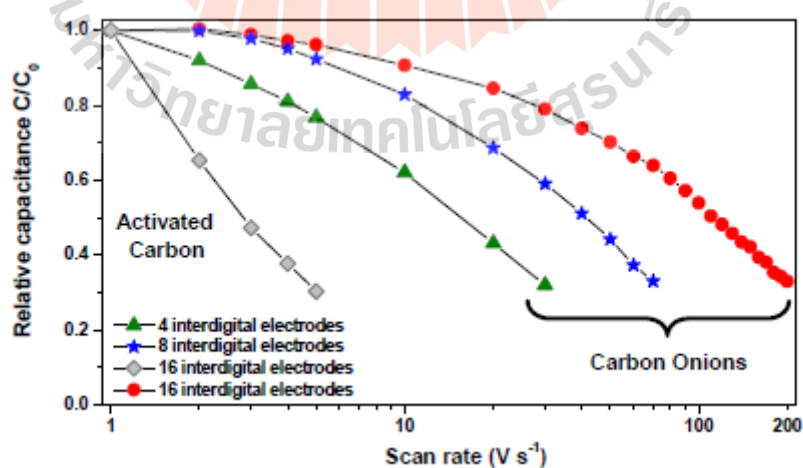


Figure 2.4 Relative capacitance for micro-devices made of 4, 8 and 16 interdigital electrodes. (Pech et al., 2010).

Systemically comparison of the performance for the conventional sandwich and planar electrode structure is conducted (Ghoniem et al., 2016). Graphene oxide (GO) film serve as an active material supported by a polyethylene terephthalate (PET) substrate . Planar electrode is patterned using high power CO₂ laser. As shown in figure 2.5, within the same controlled area, three electrode architecture of 2, 4 and 6 sub-electrode are studied. PVA-based gel electrolyte is implemented. All samples are performed the electrochemical measurement including Galvanostatic Charge/Discharge (GCD) and Electrochemical Impedance Spectroscopy (EIS). Figure 2.6 illustrates the volumetric stack capacitance with respect to the discharge current density and Nyquist plot for all samples. It is clearly observed that all planar electrodes can provide higher volumetric capacitance compared to the conventional sandwich structure. Highest capacitance is obtained from planar electrode with 6 sub-electrode (I-Ps(6)) followed by I-Ps(4) and I-Ps(2) respectively. This result indicated that the more number of interdigitate electrode per unit area, the large capacitance that can be extracted. The maximum capacitance of I-Ps(6) is increased 18 times compared to sandwich structure. Nyquist plot, figure 2.6, which measures the total resistance and ions transport behavior of the sample support the superior performance of planar electrode. Both I-Ps(4) and I-Ps(6) have much lower resistance compared to sandwich electrode as expected because of the larger number of edge fringe forming strong electric field intensity. In case of I-Ps(2), although the resistance is a bit lower and the volumetric capacitance is nearly the same as sandwich electrode, rate capability of I-Ps(2) is better. This implies the advantage of planar electrode which facilitates ions movement. For all planar samples, the line at low frequency region of Nyquist plot is about 45° to the real part axis. This also supports the efficient ions transport due to the

shorter diffuse path of the planar interdigitate configuration compared to the conventional design.

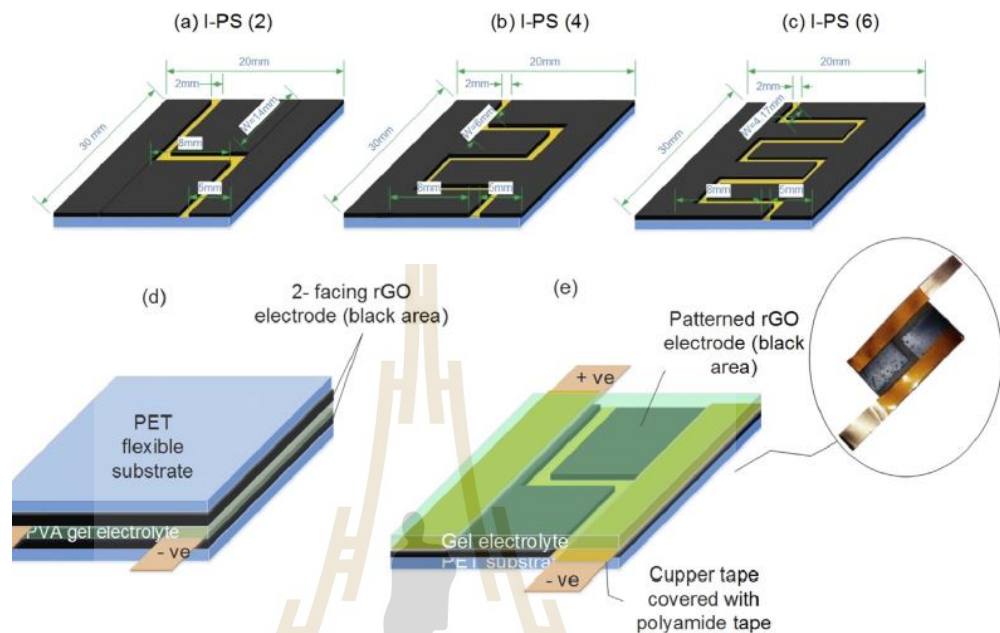


Figure 2.5 The design of in-plane electrode with a) 2 sub-electrodes I-Ps(2), b) 4 sub-electrodes I-Ps(4), c) 6 sub-electrodes, d) conventional sandwich structure and e) cell assembly. (Ghoniem et al., 2016).

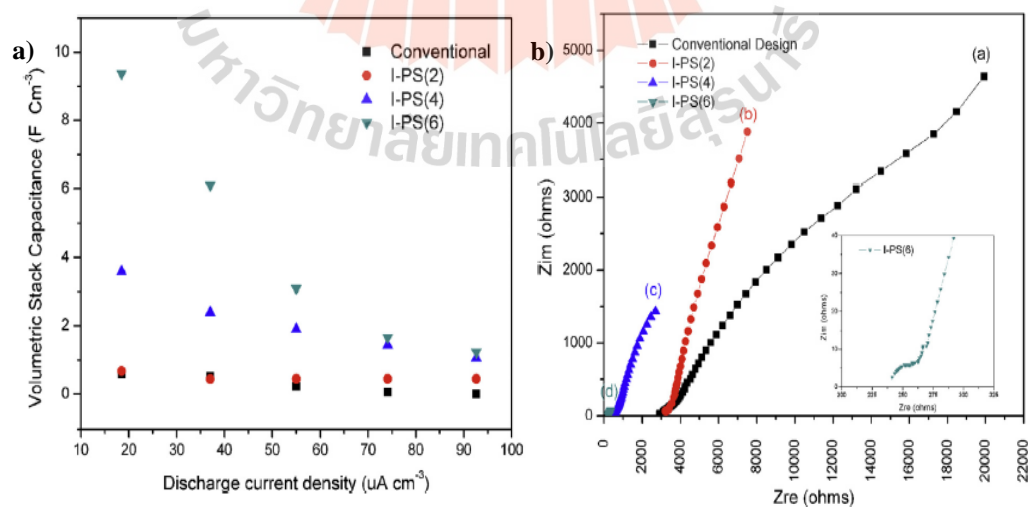


Figure 2.6 a) Volumetric stack capacitance of planar and sandwich sample and b) Nyquist plot of each sample. (Ghoniem et al., 2016).

Similar work on a comparison between planar and sandwich electrode structure has been done using all solid state graphene based fabricating by photolithography (Wu et al., 2014). The active material, graphene oxide thin film, is prepared by spin-coating on the silicon wafer. Thin layer of Au, used as a current collector, is patterned using photoresist technique. The polymer gel electrolyte of sulphuric acid –polyvinyl alcohol based is drop on the prepared electrode and left to solidify. Solid state planar electrodes are design in three difference interdigital configurations which are 32 (MSCs32), 16(MSCs16) and 8(MSCs8) electrode fingers. The optical image of all samples are shown in figure 2.7. The CV measurement is implemented at the scan rate range from 0.01 to 2000 Vs^{-1} . The stack capacitances obtained from the calculation of area within CV profile for each sample are plot with respect to the scan rate in figure 2.8. It is observed that, with in the same control area, the electrochemical performance increase with the number of interdigitate finger, in the other hand, the decrease of finger width. After 50,000 charge/discharge cycles, the sample shows about 98.5% of capacitance retention which is an outstanding cycling stability. Moreover, planar sample provide an extreme power deliver rate at 2000 Vs^{-1} while maintaining an excellent capacitance with three order of magnitude higher than conventional sandwich structure. The article indicates the influence of increasing number of electrode fringe resulting in the decreasing of average ionic diffusion path and electrolyte resistance. The result highlights the crucial role of the device architecture in determining the electrochemical performance.

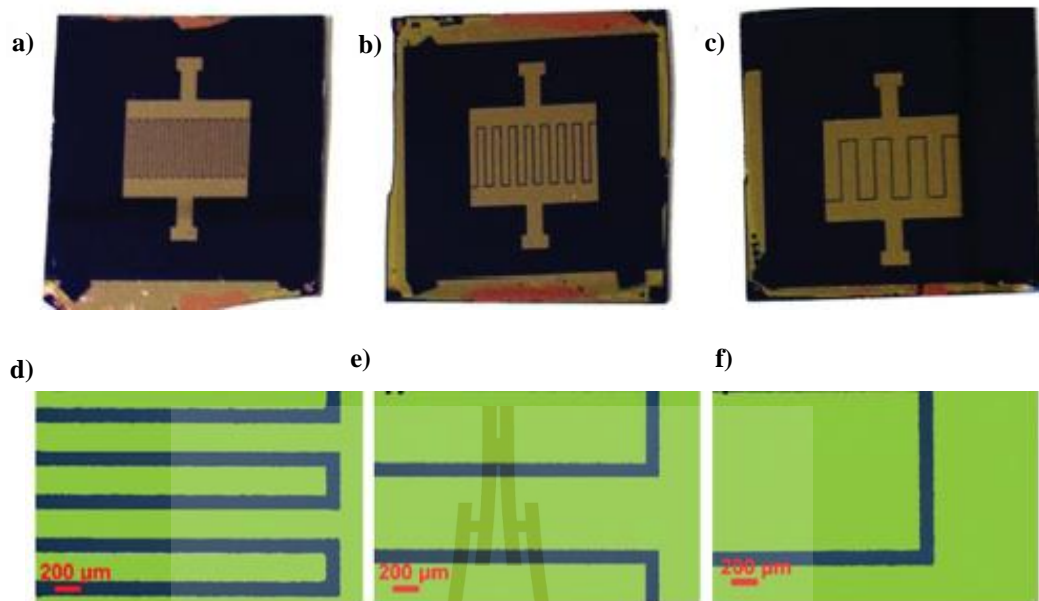


Figure 2.7 Images of micro supercapacitor(MCS) a) MSCs32, b) MSCs16, c) MSCs8 and optical image of electrode fringe (d-f). (Wu et al., 2014).

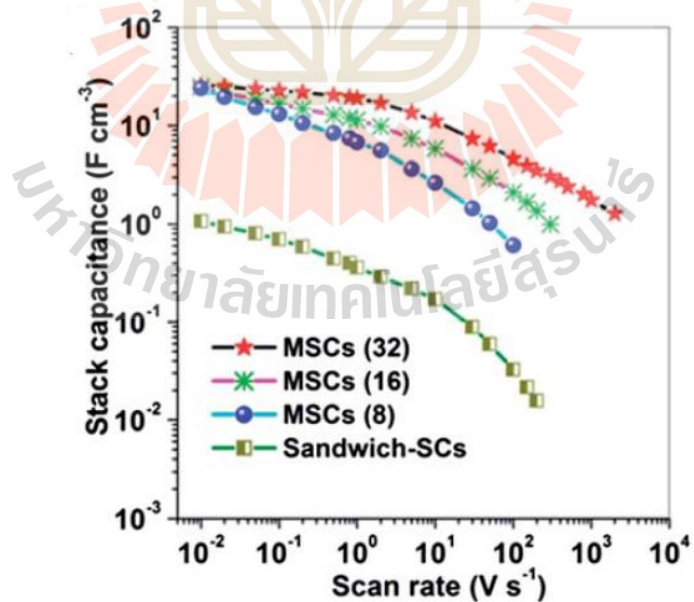


Figure 2.8 Stack capacitance of each micro and sandwich supercapacitor. (Wu et al., 2014).

2.2 Theoretical aspects

2.2.1 Simulation of electric field intensity produced by planar electrode structure

In order to theoretically understand the root causes of capacitance enhancement observed in planar electrode configuration, simulation technique is used to determine the potential gradient and electric field profile produced from each electrode pattern. This electric field effects ions movement and resistance of the cell and therefore influence the capacitance and charging performance of the device.

Figure 2.9 demonstrates the difference arrangement of electric field line between the conventional sandwich structure and planar structure electrode (Khan et al., 2015). Unlike the uniform straight electric field line of conventional parallel sandwich electrode, the electric field lines observed in planar electrode are in symmetric profile. Along the side of electrode, the straight electric field line pointing from the positive terminal to the negative terminal while on the top surface of electrode, the electric field lines are bent. The electric field intensity, obtained from 2D cross section simulation of an interdigitated electrode in figure 2.10 (Castiello et al., 2019), indicates a very high electric field intensity at the edge of adjacent planar electrode. Electric field at the field at the edge of electrode is more than twice of the electric field at the center of electrode fringe. It should be noted that the electric field profile can be manipulated by varying the electrode configuration. This edge effect is an outstanding characteristic of planar structure which leads to an enhancement of total capacitance.

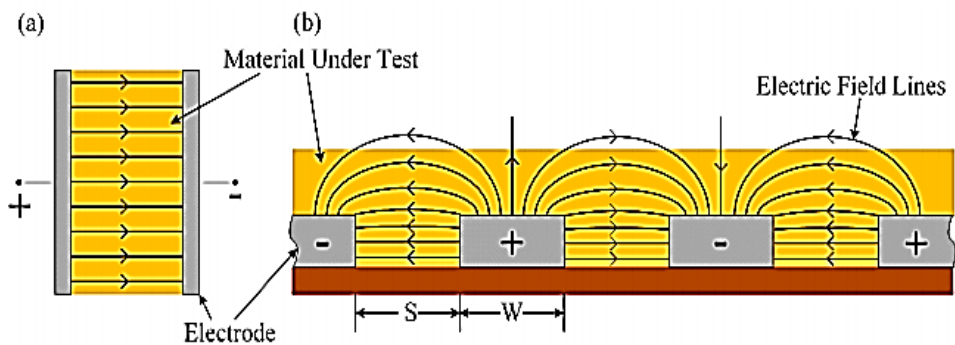


Figure 2.9 Electric field of (a) sandwich and (b) planar supercapacitor. (Khan et al., 2015).

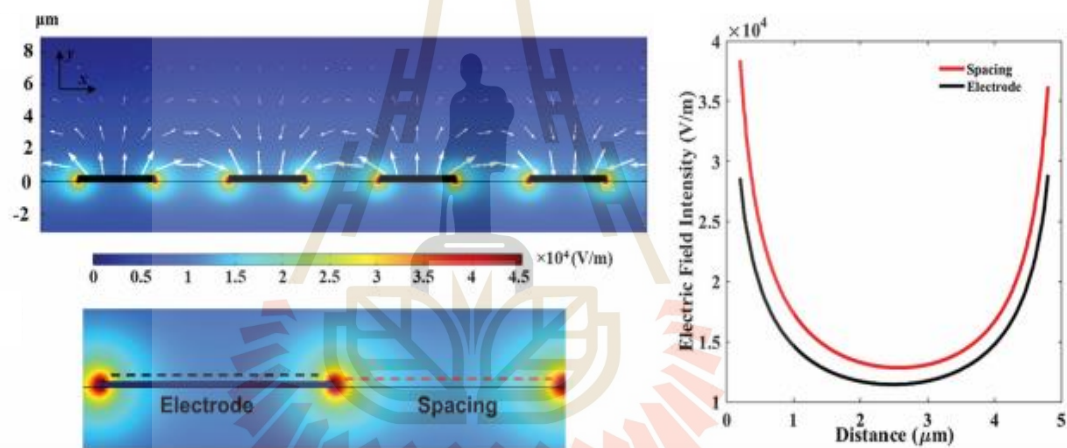


Figure 2.10 2-D cross section simulation of electric field intensity along the electrode and interspace. (Castiello et al., 2019).

Mathematical model of interdigitated electrode supercapacitor is constructed aiming to determine the dependence of capacitance on the electrode geometry. Conformal mapping technique is implemented to transform the height, width and spacing of interdigitated planar electrode into the conventional parallel plate electrode. The potential gradient within the electrolyte medium of planar electrode configuration is illustrated in figure 2.11 (Latimer et al., 2017). The simulation result found that, as

would be expected, capacitance increase with the increasing of electrode height and width but decrease with the increasing of electrode spacing.

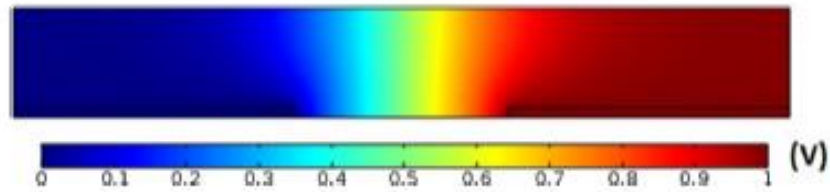


Figure 2.11 2D cross section simulation of potential distribution. (Latimer et al., 2017).

2.2.2 Dependence of electrode geometry on the cell resistance (K-cell)

By considering the resistive contribution of the electrolyte, cell constant (κ) is defined as the proportional factor between the specific resistance (ρ) of the electrolyte and the measured resistance (R) as the following equation

$$R = \kappa\rho \quad (2.2)$$

This cell constant is determined by the electrode geometry and therefore is a unique characteristic of a particular electrode configuration which effect the cell resistance regardless of electrode material (Olthuis et al., 1995). The assumptions are the thickness of electrode and the fringe end effect are neglected, the current is ohmic meaning that the current is directly proportional to the potential gradient across the plane. Since the potential gradient is very strong near the electrode, especially at the edge of electrode fringe, the resistance contribution at this point is very low. The capacitance as a function of cell constant for the planar electrode capacitor is expressed as

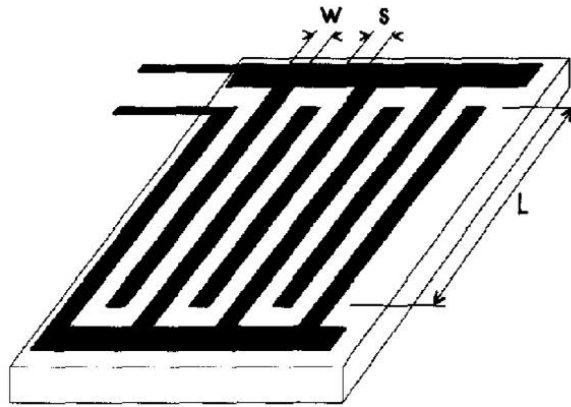


Figure 2.12 Illustration of interdigitated electrode dimension. (Olthuis et al., 1995).

$$C = \frac{\epsilon}{2} \frac{K[(1-\kappa^2)^{1/2}]}{K(\kappa)} \quad (2.3)$$

where $K(\kappa)$ is the complete elliptic integral of the first kind.

$$K(\kappa) = \int_0^1 \frac{dt}{[(1-t^2)(1-\kappa^2 t^2)]^{1/2}} \quad (2.4)$$

where $\kappa = \cos\left(\frac{\pi}{2} \frac{w}{s+w}\right)$, s and w represent the spacing and electrode width illustrated in figure 2.12 respectively.

There are an estimation of this Olthuis solution, which have been prove to be a good approximation, as shown in figure 2.13, within the range of $0.1 < S/W < 10$ while using a simplified mathematic calculation as follow,

$$K = 2 \frac{(S/W)^{1/3}}{L(N-1)} \quad (2.5)$$

where N is the number of electrode fringe.

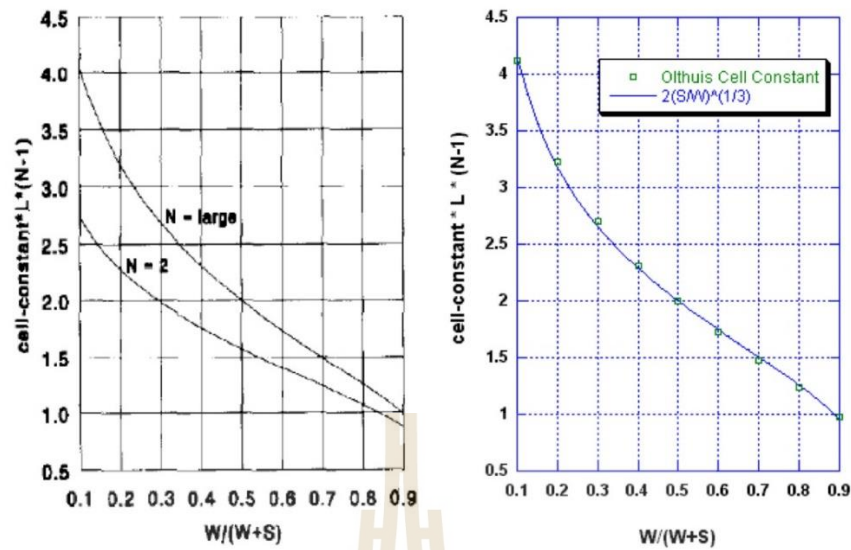


Figure 2.13 Comparison of cell constant value obtained between Olthuis *et al.* work and simplified approximation model. (Source: <http://www.mosaic-industries.com/embedded-systems/instrumentation/conductivity-meter/microfabricated-planar-interdigitated-electrodes-cell-constant>).

2.2.3 Cyclic voltammetry measurement and capacitance calculation

Cyclic Voltammetry (CV) is the most frequently electrochemical techniques used to investigate performance of supercapacitor. CV test measures the resulting current output from the applying constant rate potential sweep. This technique is typically used to acquire the information about interaction between electrolyte ions and electrode, electric double layer characteristic and redox reaction (Paula, 2015). CV curve is an outstanding tool for observing the charge/discharge voltammetry characteristic of supercapacitor. Figure 2.14 demonstrates the CV curves and their respective equivalent circuit. An ideal EDLC (figure 2.14a) shows a perfect rectangular profile while the parallelogram liked shape (figure 2.14b, 2.14c) indicates the real EDLC device. The deviation of CV shape is a result of resistive components such as

electrode material, separator and electrolyte used. For pseudo-supercapacitor, the shape of CV curve often comes up with cathodic/anodic peaks due to the Faradaic redox reaction as shown in figure 2.14d. The total capacitance can be calculated using the scan rate and its corresponding an enclosed area of CV curve.

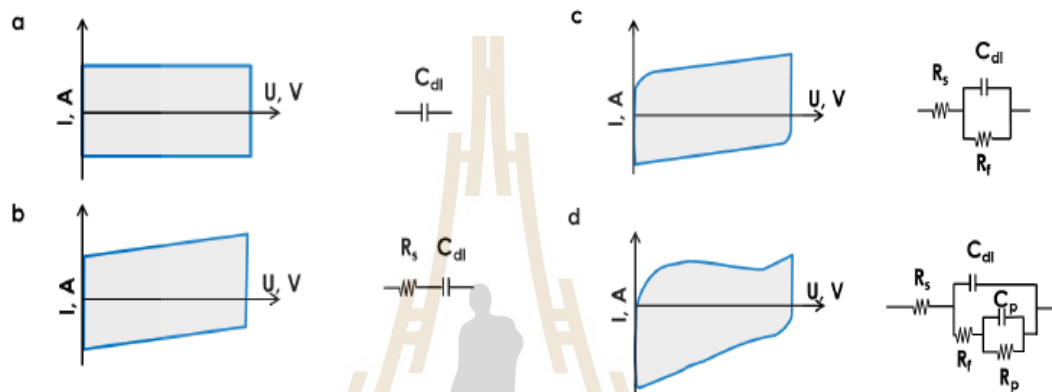


Figure 2.14 Typical voltammetry characteristic and respective equivalent circuit of a) an ideal EDLC, b) EDLC with series resistance, c) real EDLC and d) pseudocapacitor. (Paula, 2015).

CV profile obtain from any scan rate can be determined as following

From the definition of capacitance

$$Q = CV \quad (2.6)$$

$$It = CV \quad (2.7)$$

$$I = Cv$$

where Q is charge, V is applied voltage, I is current, t is time and $v = \frac{V}{t}$ is the

scan rate

$$\int_{V_1}^{V_2} I dV = \int_{V_1}^{V_2} Cv dV$$

$$\text{Area under charging curve} = Cv[V_2 - V_1]$$

Taking 2 steps of charging and discharging process

$$\text{Absolute area within CV profile} = 2Cv[V_2 - V_1]$$

$$C = \frac{\text{Absolute area within CV profile}}{2v[V_2 - V_1]} \quad (2.8)$$

2.2.4 Galvanostatic charge/discharge measurement and capacitance calculation

Galvanostatic charge/discharge (GCD), on the other hand, measures the voltage as a function of time by applying a constant current. The capacitance is calculated from the area under galvanostatic discharge current for a selected potential window. Beside the capacitance, resistance of the cell is simply obtained from the potential drop when swapping from charge to discharge process. It is normally found that the larger current applied, the larger potential drop and the lower capacitance obtained. Figure 2.15 shows the example of voltage-time profile of GCD measurement. Detail in the capacitance calculation is illustrated as following.

$$\begin{aligned} W &= Pt \\ &= (iV)t \end{aligned} \quad (2.9)$$

where W is energy, P is power, t is time, i is constant applied current and V is measured voltage.

$$\begin{aligned} W &= i \int_{t_1}^{t_2} V dt \\ W &= i(\text{area within GCD profile}) \end{aligned} \quad (2.10)$$

Since the supplied energy is equal to the energy absorbed by the supercapacitor, the capacitance of the cell can be obtained from

$$\frac{1}{2}C(\Delta V)^2 = W$$

$$\frac{1}{2}C(\Delta V)^2 = i(\text{area within GCD profile})$$

$$C = \frac{2i(\text{area within GCD profile})}{(\Delta V)^2} \quad (2.11)$$

where ΔV is the potential window

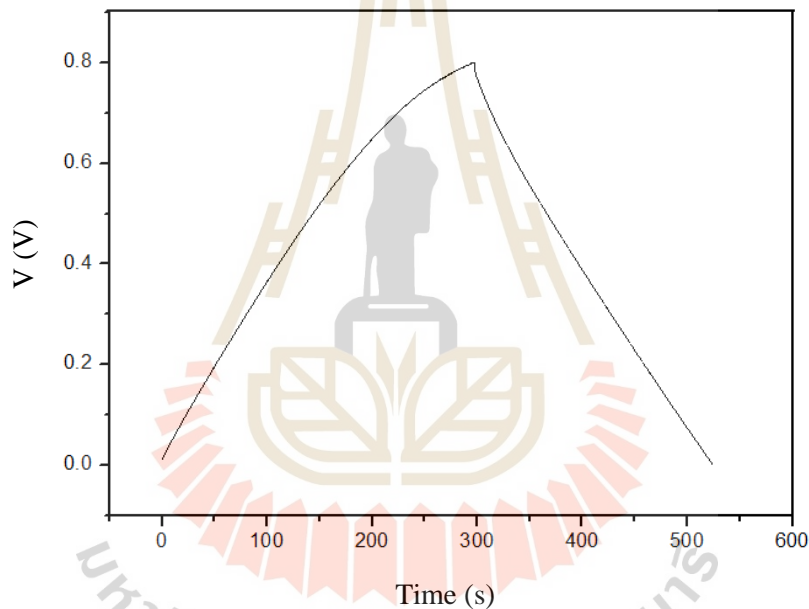


Figure 2.15 Voltage-time profile obtained from GCD measurement.

2.2.5 Electrochemical Impedance Spectroscopy

Electrochemical Impedance Spectroscopy (EIS) is a technique used to observe the frequency response behavior of capacitor by applying a small amplitude of alternating current. Nyquist plot of imaginary versus real part of impedance is the most widely used tool to indicate an equivalent series resistance (caused by electrolyte, separator and electrodes) and charge transfer resistance (developed at surface between

electrodes and electrolyte). The shape of Nyquist plot can represent the resistive and capacitive of the device as shown in figure 2.16. The Nyquist plot in figure 2.16a is the characteristic of ideal capacitor which do not have any internal resistance. The internal resistance, R_s , of the cell is in series with the capacitor as indicated by the shifted in real-part of the Nyquist plot as shown in figure 2.16b. Small semi-circle in figure 2.16c indicated the present of redox contribution of in the charge storage mechanism. EIS provides a crucial information which allow one to construct an equivalent circuit and understand the kinetic process within supercapacitor.

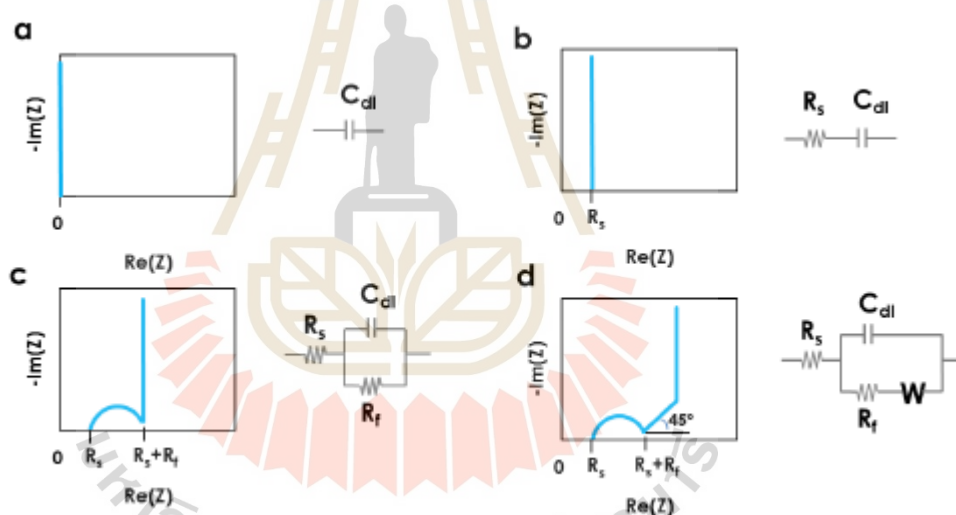


Figure 2.16 Nyquist plot of the respective equivalent circuit of a) an ideal EDLC, b) EDLC with series resistance, c) EDLC with series and parallel resistance and d) Randle circuit with Warburg impedance. (Paula, 2015).

2.2.6 Differentiation of the contribution between EDLC, redox reaction and intercalation pseudocapacitance

The electrochemical capacitor is categorized into two main groups, EDLC and

pseudocapacitor, based on its charge storage mechanism. EDLC stores electric charge at the electrode-electrolyte interface via an electrostatic force. This process occurs without any faradic reactions. During the charging/discharging process, electrolyte ions are rapidly arranged within the Helmholtz double layer. However, the amount of accumulated charge is limited by the electrode accessible surface as following.

$$C_{dl} = \frac{\epsilon A}{d} = \frac{Q}{V} \quad (2.12)$$

where C_{dl} is the EDL capacitance, A is electrode accessible surface area, d is charge separation distance at Helmholtz layer, ϵ is dielectric constant, Q is total stored charge and V is electrode potential. When the capacitor is charged with the constant potential sweep rate (scan rate), the correspond current during the charging process is

$$I = C_{dl}v \quad (2.13)$$

where v is the potential sweep rate. This equation implies the rectangular shape of CV profile obtained from EDLC energy storage mechanism. The energy density gains from EDLC is much lower than the battery. Great efforts have been implemented to enhance the energy density of electrochemical capacitor such the intruding of pseudocapacitive species.

Pseudocapacitance is the faradic process based on two sub-mechanisms which are the reversible redox reaction at the surface of electrode and intercalation of multilayer material. Redox reaction is the regular type of pseudocapacitance where the ions adsorption process takes place at the surface of electrode material such as metal oxides and conductive polymers. It should be noted that in order to allow the redox current to flow, the applied potential must greater than the threshold voltage. This voltage depends on the type of electrode material and electrolyte ion. The number of

ions that passes through the double layer and contact with the electrode surface determine the rate of reaction. The higher electrolyte concentration therefore can provide a higher redox current. Intercalation pseudocapacitance arises in 2D material occurring without any phase change. The gained capacitance depends on the electrode host structure and the intercalation ions. Intercalation pseudocapacitance is therefore a diffusion controlled which is difference from the surface controlled of EDLC and redox reaction. Unlike EDLC, the CV profile of pseudocapacitor can be in a rectangular shape with or without redox peak depending on the type of electrode and electrolyte material.

To date, there is a mathematical approach (Dunn's method) to only differentiate the contribution between slow diffusion process (intercalation pseudocapacitance) and capacitive process (EDLC and fast redox reaction) using the summation of current as a function of scan rate.

$$i(v) = i_{\text{cap}} + i_{\text{diff}} \quad (2.14)$$

where $i(v)$ is the measured current at given scan rate, i_{cap} is surface capacitive current and i_{diff} is bulk diffusion current. The capacitive contribution occurs at or near the electrode/electrolyte interface. This process linearly varies with scan rate while the diffusion contribution varies with the square root of scan rate. The summation of current can be rewritten as

$$i(v) = k_1 v + k_2 v^{1/2} = a v^b \quad (2.15)$$

$$\log i(v) = \log a + b \log v \quad (2.16)$$

where a and b are adjustable parameters while k_1 and k_2 are constants. The parameter b can be evaluated from the slope of $\log(i) - \log(v)$ plot. If the value of b nearly equal to 1, the system is dominated by capacitive EDLC and redox reaction process. If the value of b is 0.5, the system is intercalation process. Figure 2.17 shows

the electrochemical study of pseudocapacitive behavior of MXene multilayers material. The b-value is used to differentiate the contribution of surface EDLC/redox and bulk intercalation contribution (Shao et al., 2019). The charge storage mechanism deviates from EDLC/redox at low scan rate to intercalation pseudocapacitance at higher scan rate indicating by the b-value changing with the applied scan rate. At the scan rate range between 1 to 10 mV/s, b-value is 1 which implies the pure capacitive behavior while at higher scan rate, b-value becomes lower which indicates an increase of intercalation contribution. The proportion of surface and bulk process are illustrated in figure 2.18. The surface process dominates at high scan rate as expected because it is a rapid storage mechanism which the bulk process takes some diffusion time. As the scan rate is increased, the bulk intercalation pseudocapacitance decreases as shorten of the diffusion time.

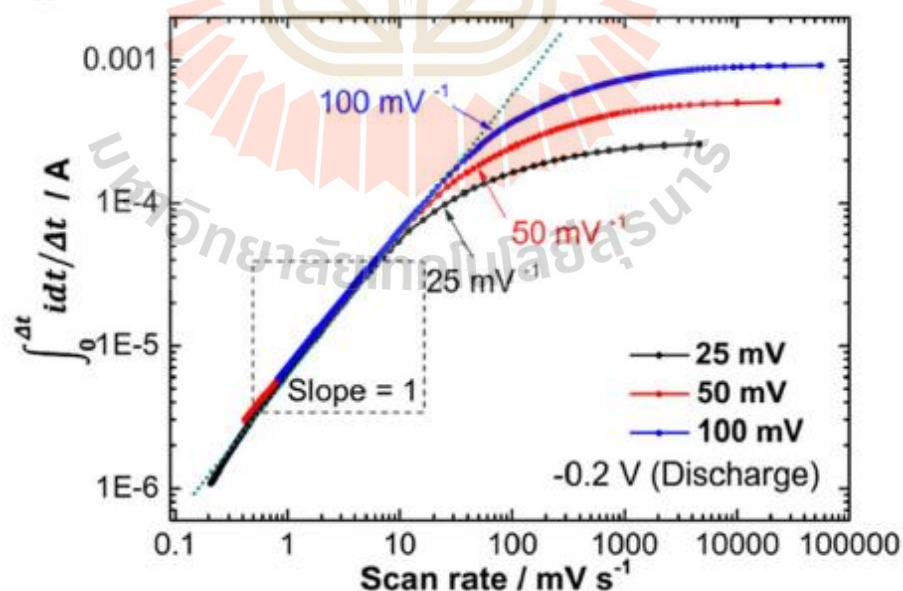


Figure 2.17 The b-value with respect with scan rate of Mxene multilayer material. (Shao et al., 2019).

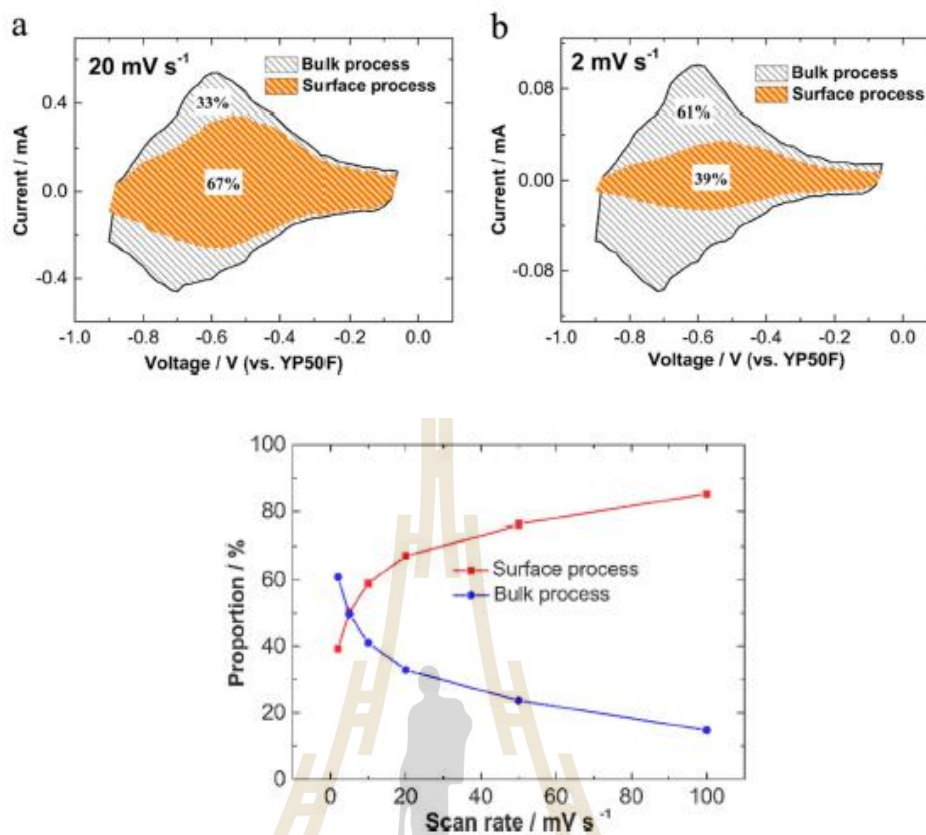


Figure 2.18 The CV profile at a) 20mV/s, b) 2mV/s and the contribution of surface and bulk process on the total capacitance. (Shao et al., 2019).

It should be noted that the contribution between surface (EDLC/redox) and bulk (intercalation) can be differentiated by the method mentioned above. Unfortunately, the contribution of EDLC and redox reaction cannot be easily do because they share the same response behavior with the applied scan rate.

CHAPTER III

METHODOLOGY

In this section, the methods of electrode fabrication are illustrated. The first step is to systematically design electrode pattern. The procedure of compounding carbon ink and electrolyte are explained. The coating process, preparing final sample and also the experimental setup are summarized. At the end of chapter, potential gradient and electric field intensity simulation and modelling setup of the planar electrode using COMSOL Multiphysics is demonstrated.

3.1 Electrode fabrication

3.1.1 Current collector design and fabrication

The planar current collector used in this work are gold coated printed circuit board (PCB). The periodic comb-like planar electrode patterns are used as a studied case. As illustrated in figure 3.1, there are three different planar electrode configurations and the conventional sandwich electrode. The width of planar electrode fringe is varied from 2 mm, 3 mm and 4 mm which designated as type 2, type 3 and type 4 respectively. The interspace gap between adjacent electrodes is fixed at 1 mm. It should be noted that too small interspace gap may cause the short circuit across the adjacent electrode due to the high electric field intensity at the edge of electrode fringe. All sample are patterned within the same control area of 30×60 mm. Note that the

narrower of electrode width, the larger number of electrode fringe. Since the gap space at the end of each electrode fringe is very small compared to the length of the fringe, the fluctuation of electric field at the end of the fringe can be neglected. The conventional sandwich structure electrode is a fully gold coated electrode within the same control area. The pattern PCB is used as received without any further treatment.

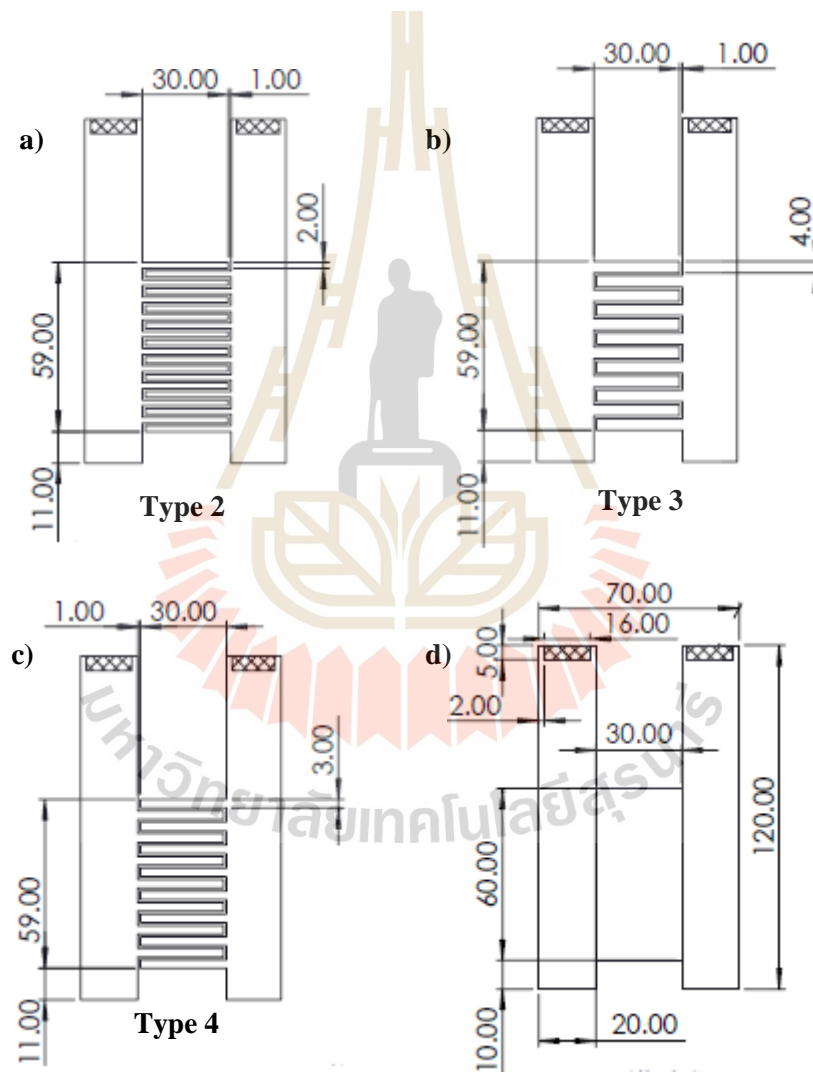


Figure 3.1 Schematic of planar electrode of a) Type 2 (2 mm.), b) Type 3 (3 mm.), c) Type 4 (4 mm.) fringe width and d) sandwich structure.

3.1.2 Active material and electrolyte preparation

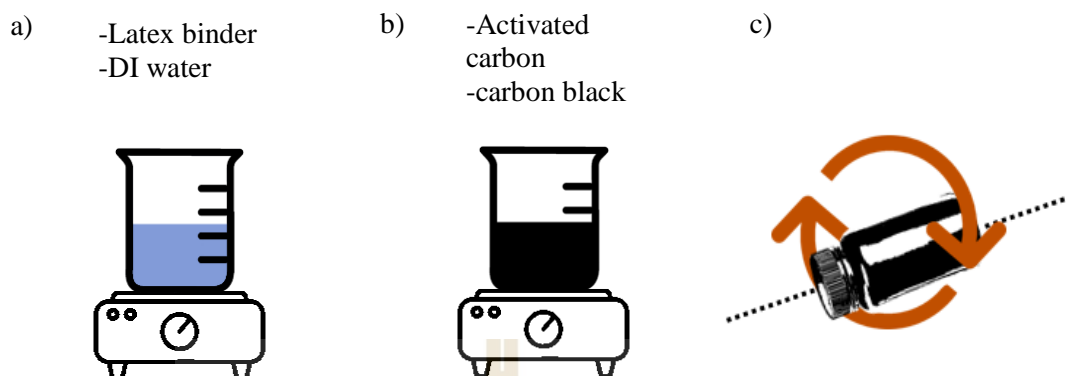


Figure 3.2 Active material preparation process of a) pre-mixed binder, b) Carbon ink and c) ball mill.

Since the objective of the research is to investigate the influence of electrode configuration on the performance of supercapacitor, the active material used here is a common material usually implement in supercapacitor area which are activated carbon, carbon black and latex binder. Activated carbon provide a very large surface area which electrolyte ions can be attached. The small portion of carbon black is added in order to increase the conductance of the overall active material. Firstly, latex binder (5 g) and DI water (20 ml.) are mixed together. The dissolved binder is stirred at room temperature for 30 minutes. Activated carbon (9 g) and carbon black (1 g) are added into the prepared binder. The carbon ink is continue stirring at 60°C for 2 hours and then put into ball-mill machine at 500 rpm for 24 hours as illustrated in figure 3.2. Sodium nitrate, neutral electrolyte, obtained from 99% assay grade of sodium nitrate (Sigma-Aldrich S5506) is used as an ions electrolyte medium. Sodium nitrate is a water based electrolyte which provides higher ions mobility than organic electrolyte. This high ions mobility is preferred for planar electrode configuration.

3.1.3 Coating process and cell assembly

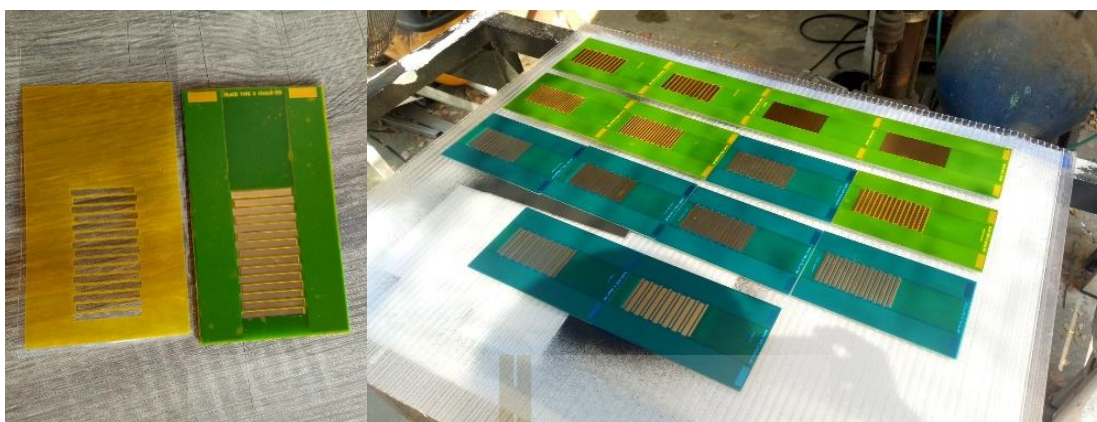


Figure 3.3 Schematic of printed circuit board cover with remove sticker mask for coating process.

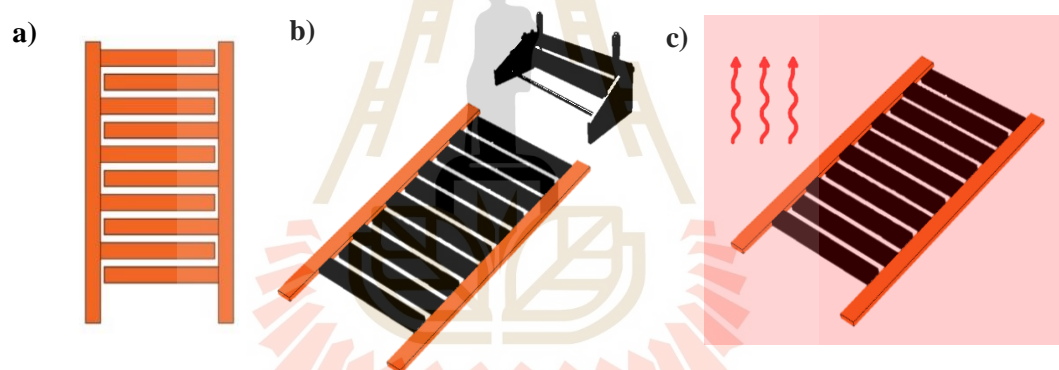


Figure 3.4 Coating process a) electrode, b) doctor blade coating and c) drying process.

In order to patterned coat the current collector with carbon ink, the PCB is covered by sticker mask as shown in figure 3.3. The carbon ink is then coated on the pattern PCB using doctor blade machine. The sticker mask is removed and the coated electrode is dried at room temperature for 2 hours. The sample is put into an oven at 150°C for 1 hour and left until is cooled down to the room temperature as shown in figure 3.4. Similar to the planar patterned electrode, the sandwich electrode which is used as a reference conventional configuration is fabricated with the same procedures. The carbon ink is fully coated within the control area.

3.2 Electrochemical measurement

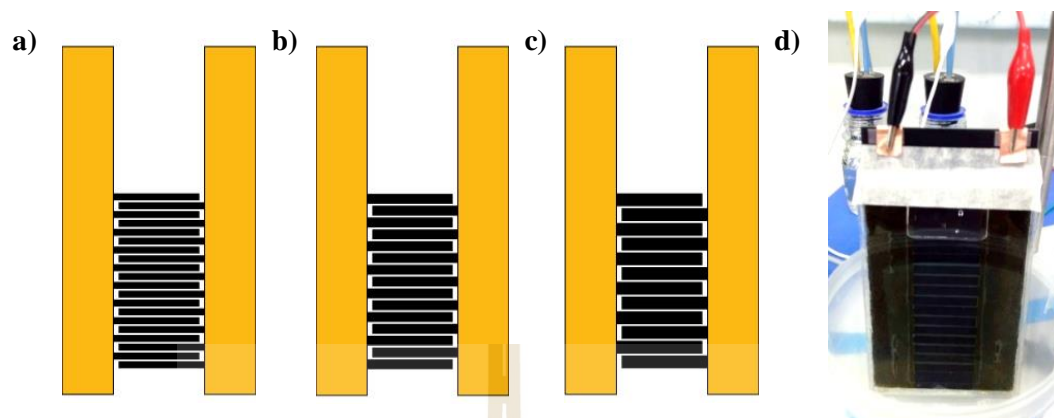


Figure 3.5 Planar electrode supercapacitor with array ratio of a) 2:1, b) 3:1, c) 4:1 and d) real two electrode system set up.

The prepared samples, shown in figure 3.5, are insert in the 3D printing case and filled with electrolyte. The entire unit is sealed to prevent any disturbance. Two-electrode system using Metrohm-Autolab potentiostat/galvanostat is set for CV measurement. Scan rate is varied from 2 to 200 mV/s and cutoff potential is set to be 0.8 V in order to prevent water molecule decomposition. Note that even the aqueous electrolyte provides relatively high ions mobility, but the applied voltage is limited around 1.23 V. The measurements take place in ambient air at room temperature. Measured data is recorded and analyzed using Nova 2.1 software. For each scan rate, the process is run for three cycles to make sure that the system is stable indicated by the same CV profile obtained from each cycle. The measured data is collected from the last cycle of each scan rate. The capacitance is calculated from area within CV profile, figure 3.6, as explained in chapter 2.2.3 Cyclic Voltammetry and capacitance calculation.

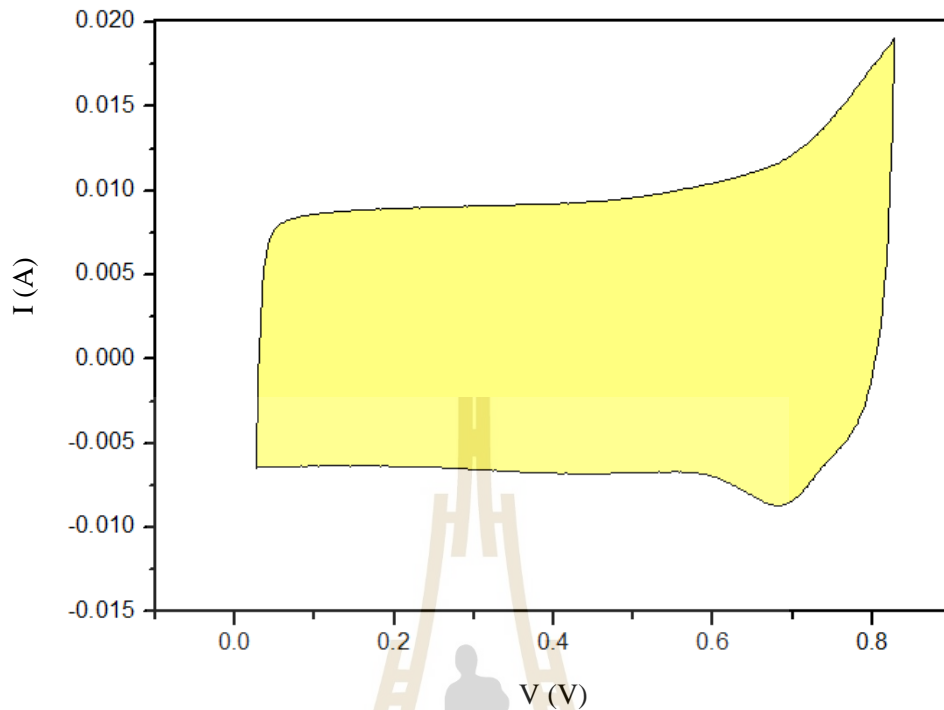


Figure 3.6 CV profile of type 2 planar electrode at scan rate of 100 mV/s.

3.3 Electric field simulation

In order to verify the influence of electrode configuration on the performance of supercapacitor, COMSOL Multiphysics is introduced to simulate the potential gradient and average electric field intensity produced by each electrode pattern. COMSOL is the well-known mathematical modeling software used in many areas of physics, engineering, manufacturing and scientific research. To specifically determine the potential gradient and electric field intensity, the AC/DC electrostatic model wizard window is selected. The stationary study mode is used. In order to determine the electric field intensity, the Poisson differential equation is solved using finite element method as following.

$$\nabla^2 \psi = f(\vec{r}) \quad (3.1)$$

where $f(\vec{r})$ is a density of field source

The equation is satisfied when the solution with the minimized total energy is reached. Firstly, the approximation for the solution is initiated by parameterizing the guess solution $u(x)$ into $u_{u1,u2,\dots,u(n-1)}(x)$. Then the expressions for the total energy of the system are derived in terms of parameter u_1, u_2, \dots, u_{n-1} . Each solution element is approximated by a polynomial function. Finally the value of parameters that provide the minimum total energy is determined.

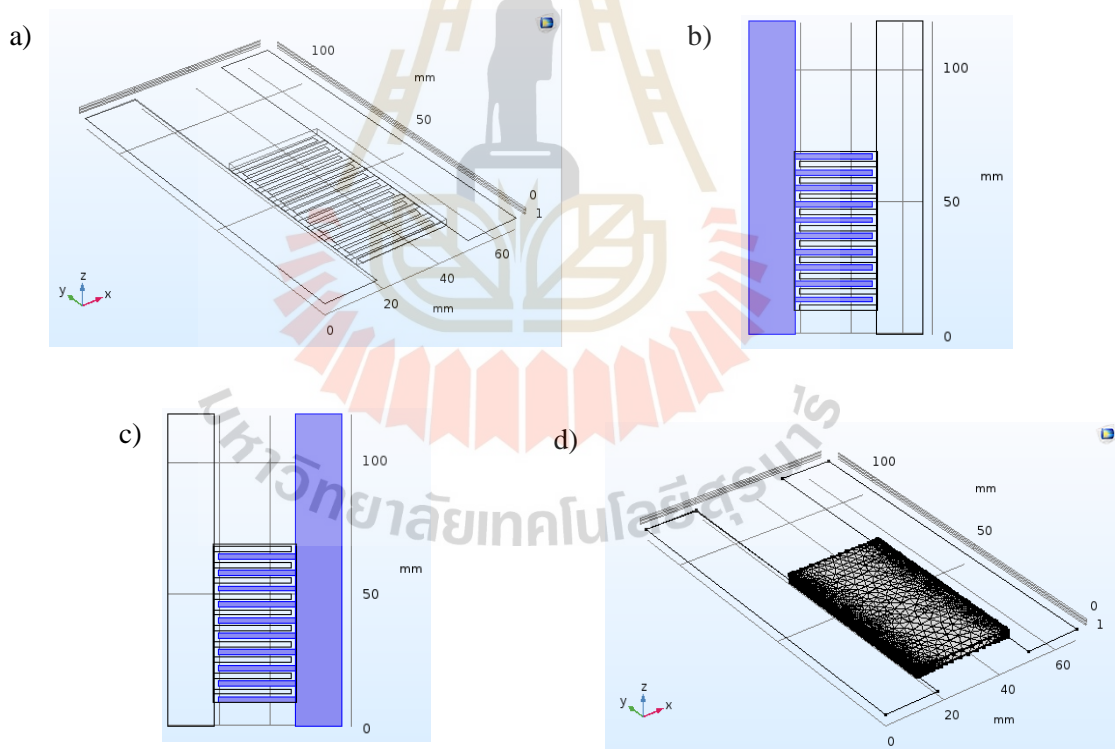


Figure 3.7 COMSOL simulation a) electrode geometry, b) ground boundary, c) terminal boundary and d) meshing of model domain.

There are four simulation steps carried out in COMSOL. First step is to build the geometry. In this step, one need to define the location of the considered object. It can be 1D, 2D or 3D object. The coordinate can be Cartesian, polar or cylindrical. Second, one need to define models, material properties and boundary conditions. The define model is to select the partial differential equation to be solved. The material properties are, for example, dielectric constant and the conductivity. Boundary conditions can be the specified voltage or charge at the boundary. Third step is to mesh the model. Meshing the model is the numerical way to solving the partial differential equation. The strategy is to break the model into a very tiny piece called element. The Poisson equation is then solved within each element. The finer mesh model provides the better accuracy of the calculation. The last step is results and post processing. In this step, one may add the color, arrow or plot to illustrate the calculation result.

As Shown in figure 3.7, the metal electrode is sketched up in real scale according the planar electrode type 2, type 3, type 4 and also conventional sandwich structure. The metal electrode fringes, assigned as a copper electrode, on the left are set as the ground boundary while on the right are set as the terminal boundary. The layer of conductive electrolyte with the relative permittivity of 8.6 is put on the top of pattern electrode as the model domain. The modelling mash is set to extra fine level in order to obtain an accurate result. Figure 3.8 show the potential gradient across each electrode by applying 0.8V to the terminal electrode with respect to ground electrode. The electric field at difference layers within conductive electrolyte along the lateral cross section is plotted in figure 3.8. The electric field profile illustrates the smooth and excellent periodic pattern.

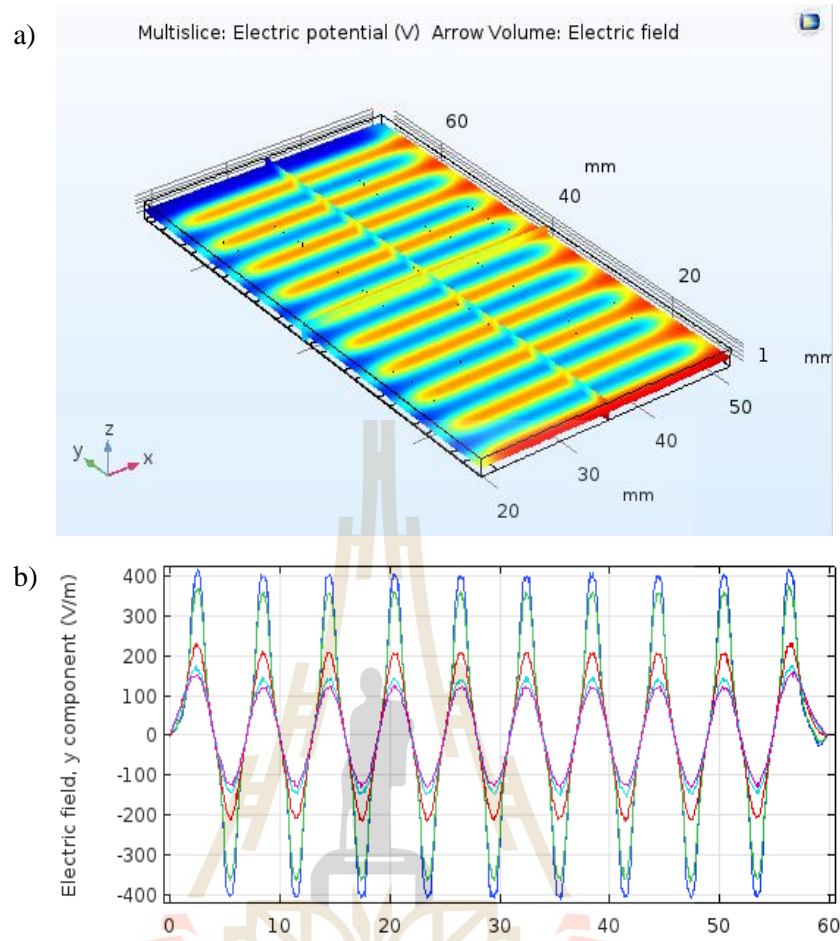


Figure 3.8 COMSOL simulation a) potential gradient and b) electric field intensity of the planar electrode.

CHAPTER IV

RESULTS AND DISCUSSION

In this chapter, the specific capacitance and rate capability of all samples obtained from the CV measurement is illustrated as a function of applied scan rate. The potential gradient, electric field intensity and cell constant for each electrode configuration is determined in order to support the capacitance results. The approach of the differentiation between EDLC and redox contribution on the total capacitance is initiated using the mapping CV profile technique. The related parameters are discussed aiming to provide a general guideline to determine and control optimum charging rate.

4.1 Specific capacitance and rate capability profile

4.1.1 Specific capacitance of planar and conventional sandwich structure with respect to scan rate

Specific capacitance as a function of scan rate for the sample with conventional sandwich and planar structures are illustrated in figure 4.1. Both samples are submerged in sodium nitrate electrolyte. The capacitance is calculated using area within CV profile. The maximum specific capacitance of planar electrode is 22.03 Fg^{-1} which is 86.7% higher than the conventional sandwich structure (11.80 Fg^{-1}). It can be clearly seen that the specific capacitance of all planar electrodes are significantly higher than the conventional sandwich structure for all range of applied scan rate.

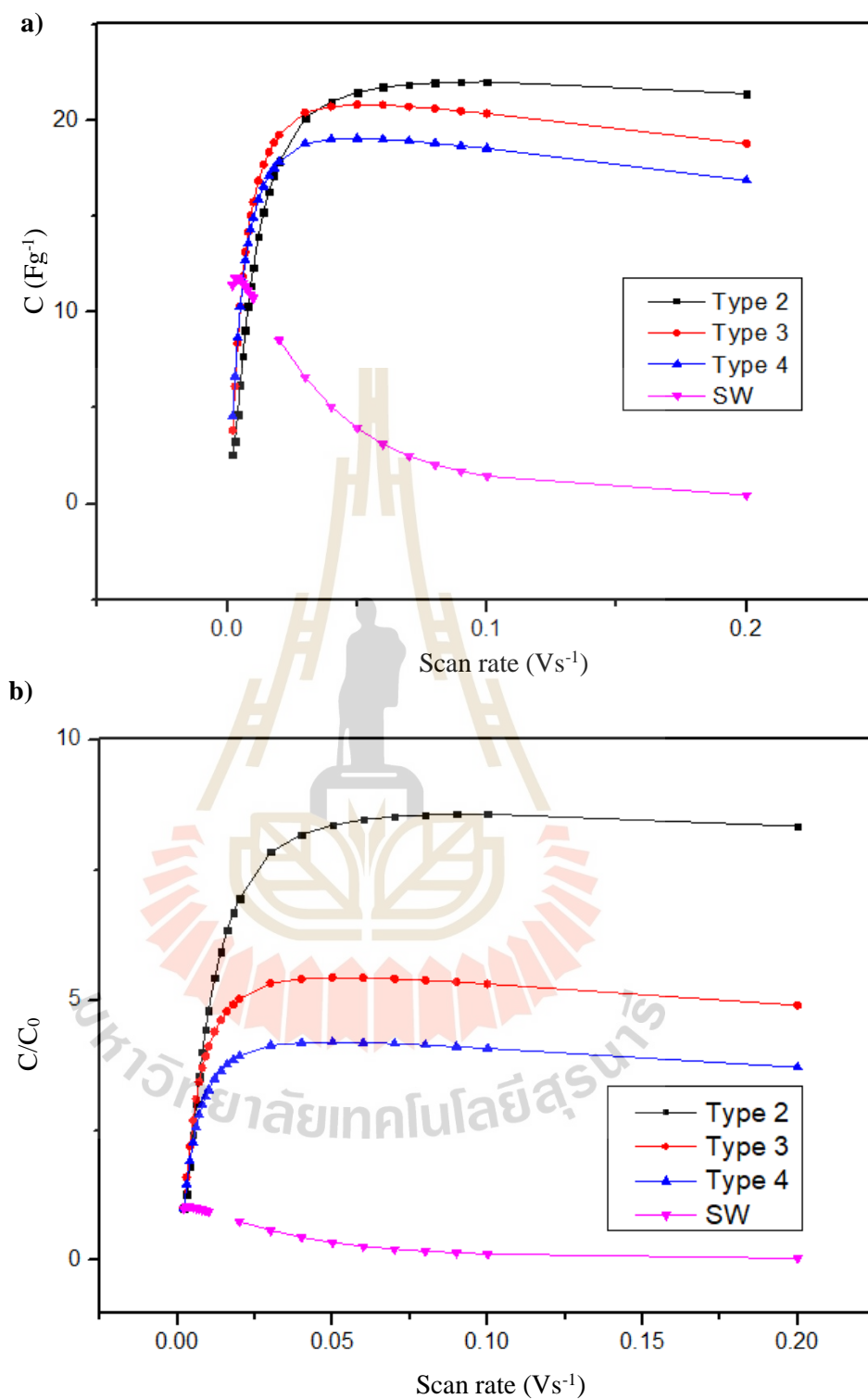


Figure 4.1 a) Specific capacitance with respect to scan rate of each sample and b) Relative capacitance with respect to scan rate of each sample.

In spite of difference active material coated area (full area coated for sandwich and pattern coated for planar structure), the specific capacitance (total capacitance of the sample divided by the mass of carbon-based material used) still represents a fair comparison of these two structures because the capacitance do not depend on the coated area but depends on the total surface area of the electrode which is already taken into account by the carbon-based material mass. The increasing of capacitance with respect to charging rate is a very interesting and crucial behavior because it allows us to improve the performance of energy storage device which will facilitate the high power and high energy density at the same time. In order to further confirm this behavior, the galvanostatic charge/discharge (GCD) technique was also carried out. This technique, opposite to CV, apply the constant charging and discharging current while measuring the corresponding voltage occur. GCD profile and the calculated capacitance are shown in figure 4.2 and 4.3 respectively.

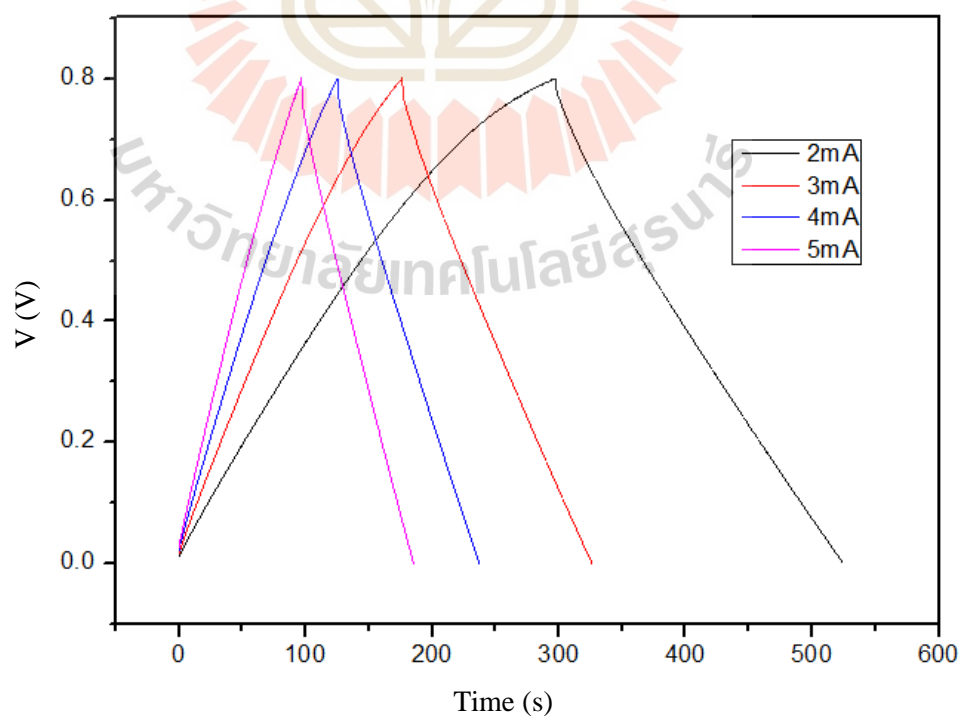


Figure 4.2 GCD profile with varying discharging current.

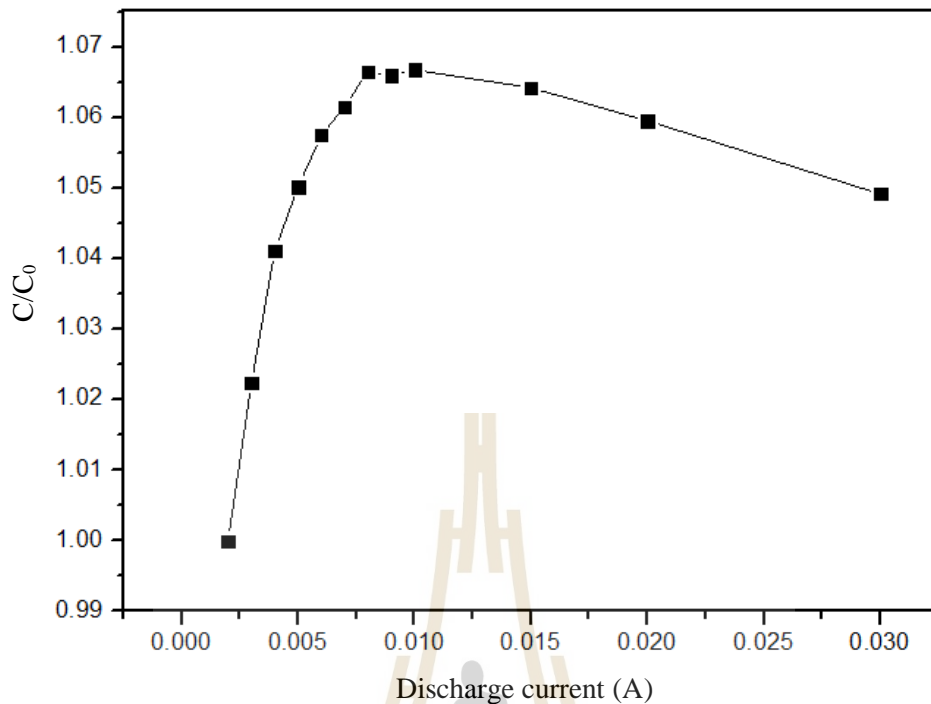


Figure 4.3 Relative capacitance with respect to discharging current obtained from galvanostatic charge/discharge measurement.

Indicate from the triangular shape of GCD profile, the measured cell shows good capacitive characteristic of supercapacitor with a small amount of IR drop. Relative capacitance with respect to discharging current in figure 4.3 confirms the increasing of the capacitance with respect to charging rate obtain from both CV and GCD measurement. Throughout further analysis, only CV measurement will be carried out because this technique can provide more information of charging mechanism and interaction between electrolyte ion and electrode than GCD measurement.

4.1.2 Potential gradient and average electric field intensity simulation results

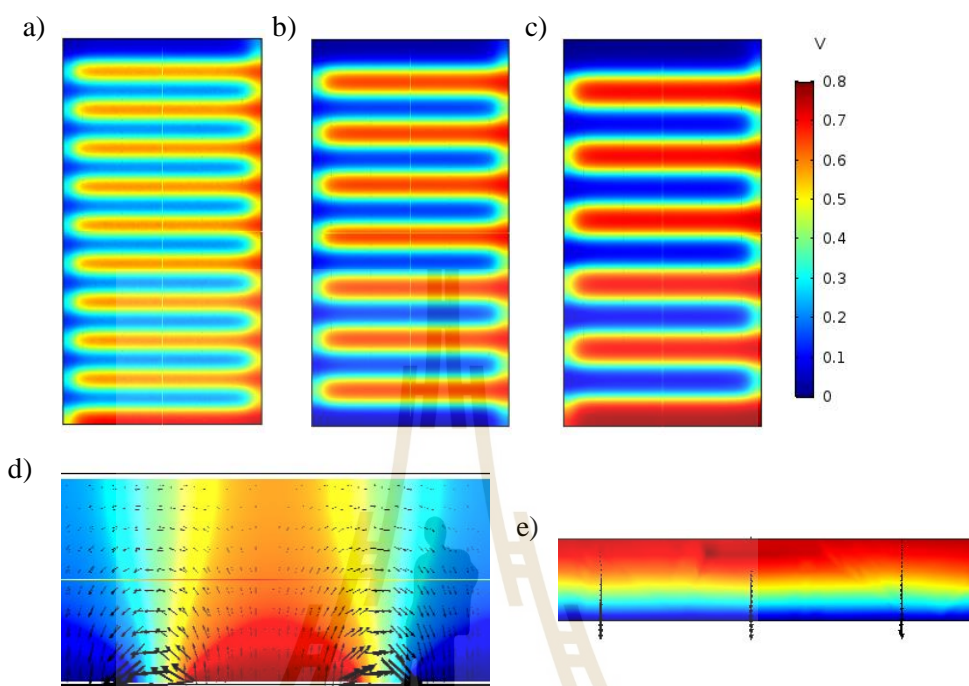


Figure 4.4 Potential gradient of planar electrode with a) 2mm, b) 3mm and c) 4mm fringe width. Electric field line of d) planar and e) sandwich structure.

Figure 4.4 shows simulation profile, using COMSOL Multiphysics, of the potential gradient and electric field lines for each sample. The average electric field of planar structure is higher than the sandwich type as shown in table 1, especially at the edge of electrode fringes. Trend of both maximum specific capacitance and average electric field intensity are in good agreement. The narrowest electrode fringe width provide the highest electric field and highest capacitance. It is also found that, in figure 4.1, even the scan rate was increased 100 times (up to 200 mVs^{-1}), the specific capacitance of the planar sample is still higher than its initial value, C_0 , (at 2 mVs^{-1}) while in case of sandwich type, the dramatic capacitance reduction is observed. This is

an unusual rate capability for supercapacitor because the specific capacitance trend to decrease with an increase of scan rate due to the electrolyte ions mobility limit. The specific capacitance enhancement observed here therefore may cause by the effect of electrode layout which indicates the advantage the planar electrode structure.

Table 4.1 Maximum capacitance from CV measurement, average electric field intensity from COMSOL simulation and cell constant for each sample.

| Sample | Maximum Specific Capacitance (Fg⁻¹) | Average Electric field (Vm⁻¹) | Cell constant (K-cell) (m⁻¹) |
|---------------|---|---|--|
| Type 2 (2 mm) | 22.03 | 162.58 | 0.0028 |
| Type 3 (3 mm) | 20.83 | 156.04 | 0.0033 |
| Type 4 (4 mm) | 19.07 | 140.66 | 0.0038 |
| Sandwich (SW) | 11.80 | 28.57 | - |

Following the approximation of Olthuis solution, the cell constant (K-cell) of each planar sample can be determined using equation 2.5. This cell constant represent the resistance nature of the electrode configuration. The higher cell constant, the higher cell resistance. As illustrated in table 4.1, the cell constant is in good agreement with the calculated average electric field results. The higher electric field intensity which observed in the narrower electrode width, the lower cell constant and therefore lower cell resistance. The calculated result of both electric field intensity and cell constant are as expected because the narrow electrode fringe width is likely to provide the high electric field and low resistance (low K-cell).

4.2 Differentiation between EDLC and redox reaction contribution on the total capacitance

4.2.1 Specific capacitance of planar electrode using varied electrolyte concentration

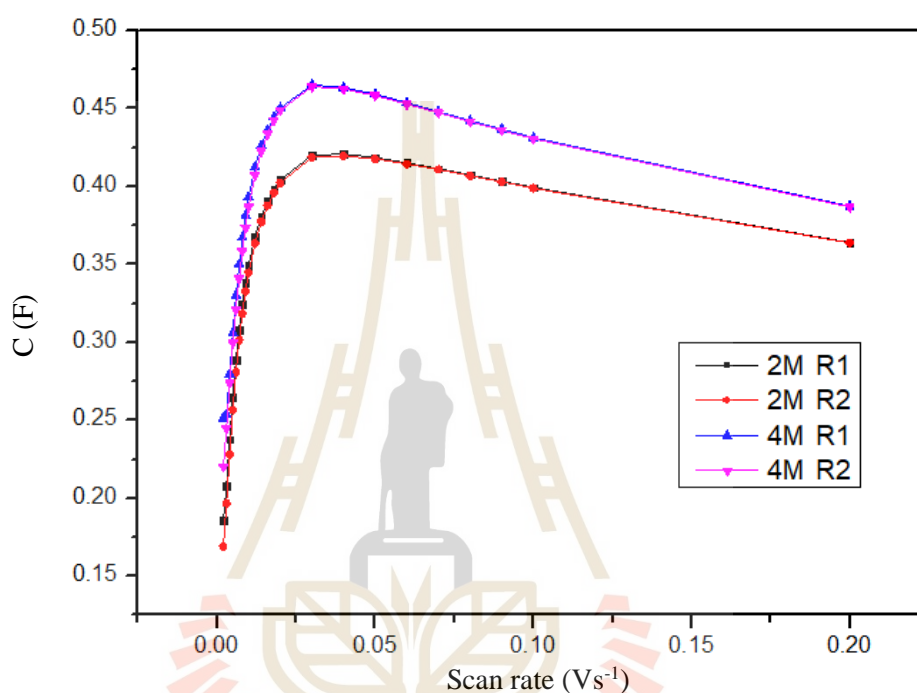


Figure 4.5 Capacitance with respect to scan rate of planar electrode in 2M and 4M sodium sulfate electrolyte.

To investigate the ions storage behavior of planar structure, CV measurements are carried out with difference electrolyte concentration condition. The scan rate is varied forward (R1) and backward (R2) between 2 to 200 mVs⁻¹ to ensure the consistency of measured data. Figure 4.5 shows an average specific capacitance with respect to scan rate of planar electrode submerging in 2M and 4M sodium nitrate electrolyte. Similar trend of rate capability profile are observed for both conditions. Higher electrolyte concentration provides the higher specific capacitance as expected because there are larger amount of electrolyte ions in the system. The maximum peak

value of specific capacitance occurs at nearly the same scan rate applied (around 30-40 mVs^{-1}) which indicates the unique characteristic of electrode geometry regardless of ions concentration.

4.2.2 CV profile mapping technique

CV profile at varied scan rate for both 2M and 4M concentration conditions are illustrated in figure 4.6. For the entire range of scan rate (2-200 mVs^{-1}), the area under CV profile, which determines the capacitance, of 4M condition are always greater than 2M condition as expected because there are larger amount of ions in electrolyte. It is clearly observed that at 200 mVs^{-1} (fast charging rate), the shape of CV profile for both conditions are rectangular which implies the characteristic of EDLC while at 2 mVs^{-1} (slow charging rate), CV profiles show some peak and bump indicating that there is redox reaction involved in charge/discharge process. This behavior can be explained by the fact that pseudocapacitance from chemical redox reaction requires lengths of completion time while pure electrostatic force attraction in EDLC is a rapid process. The CV profile is therefore point out the redox contribution at low scan rate (large charging period for complete many redox cycles) and gradually converged to rectangular EDLC shape at high scan rate. By carefully considering the shape of CV profile for both conditions, it is found that there is a region which these profiles are perfectly superimpose as the shaded area in figure 4.6. The overlapped area is rectangular shape which corresponds to the contribution of EDLC on the total capacitance. The result implies that, at each scan rate, difference electrolyte concentration provides the same amount of EDLC contribution. Even there is more than enough ions in electrolyte but EDLC is surface area dependence charge storage mechanism, the contribution is therefore limited because surface area of active material

is fixed. The excess ions only provide the additional contribution of pseudocapacitance which depends on the amount of ions in electrolyte. This overlapped area increases with the applied scan rate because, as mention earlier, EDLC is dominated in fast charging process.

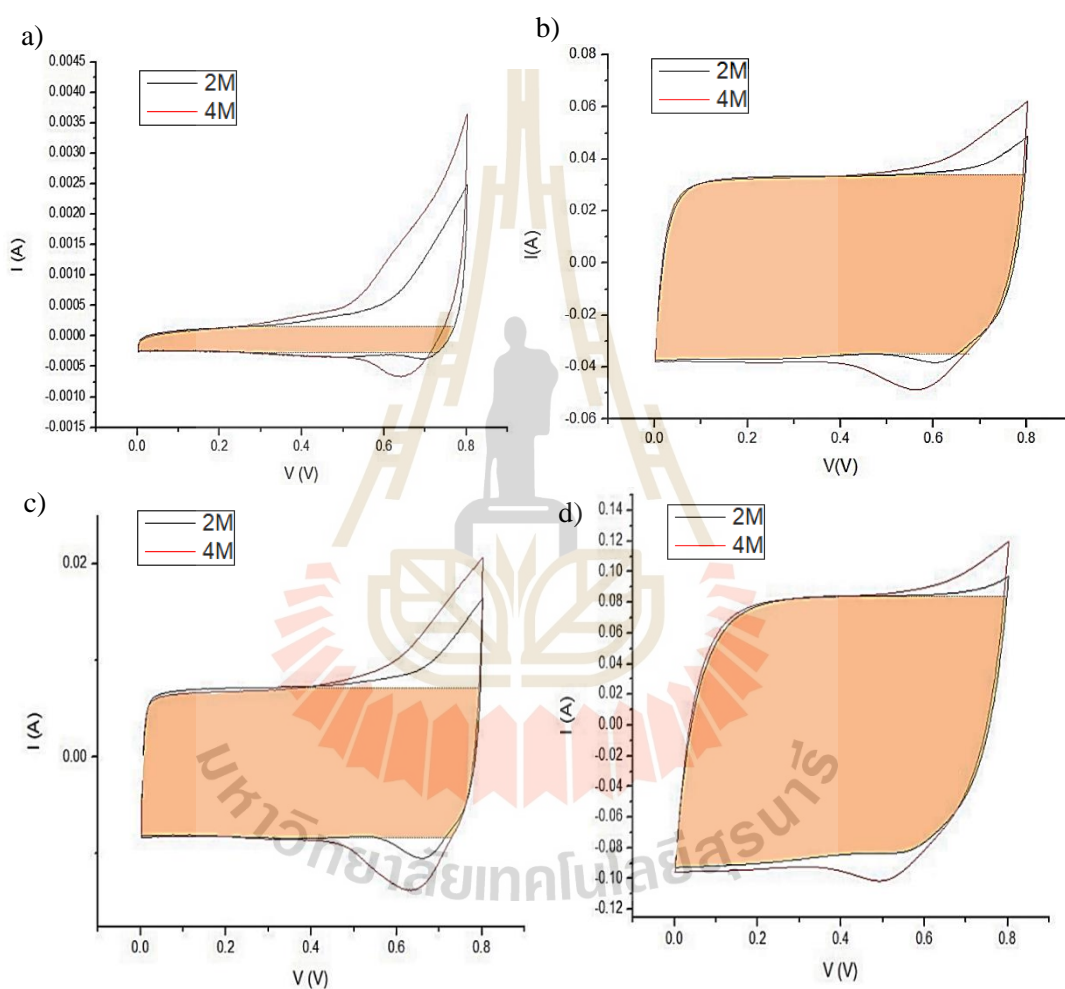


Figure 4.6 CV profile of planar electrode in 2M and 4M sodium sulfate electrolyte at scan rate of a) 2 mVs^{-1} , b) 20 mVs^{-1} and c) 80 mVs^{-1} and 200 mVs^{-1} .

Since the activated carbon and carbon black which are the active material of the electrode are used as received without any treatment or purification, it is suspected that the small amount of redox contribution is caused by some functional group that may attach to the carbon. In order to verify the present of redox pseudocapacitance, the sample is therefore taken into Electrochemical Impedance Spectroscopy (EIS) measurement. EIS is the technique that apply the small amplitude of AC signal at varying frequency and measures the corresponding voltage or current. The measurement is at 0.8V with the frequency range from 10 to 10,000 Hz.

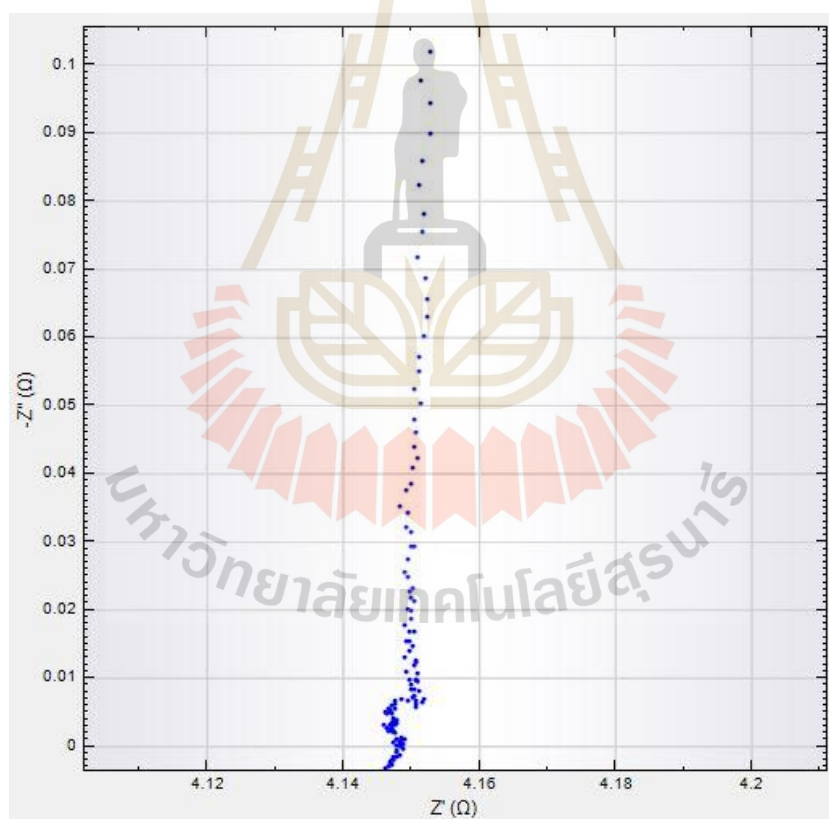


Figure 4.7 Nyquist plot of the cell using carbon-based electrode and sodium nitrate electrolyte.

The Nyquist plot in figure 4.7 provides the information about the real-part and imaginary-part of the cell resistance. The small semi-circle of the obtained Nyquist plot indicates the present of some chemical redox contribution in the charge storage mechanism. The almost vertical trend of the plot also indicates a good capacitive behavior of the cell.

To the best of our knowledge, there is a mathematical analytic method to only distinguish between the surface (EDLC and redox reaction) and bulk (intercalation of sheet material) contribution from the total capacitance. Following the equation 2.13, the average b-value obtained from the slope of $\log(i)$ vs $\log(v)$, shown in figure 4.8, is around 1.02. The result implies that there is only surface contribution in this activated carbon base material.

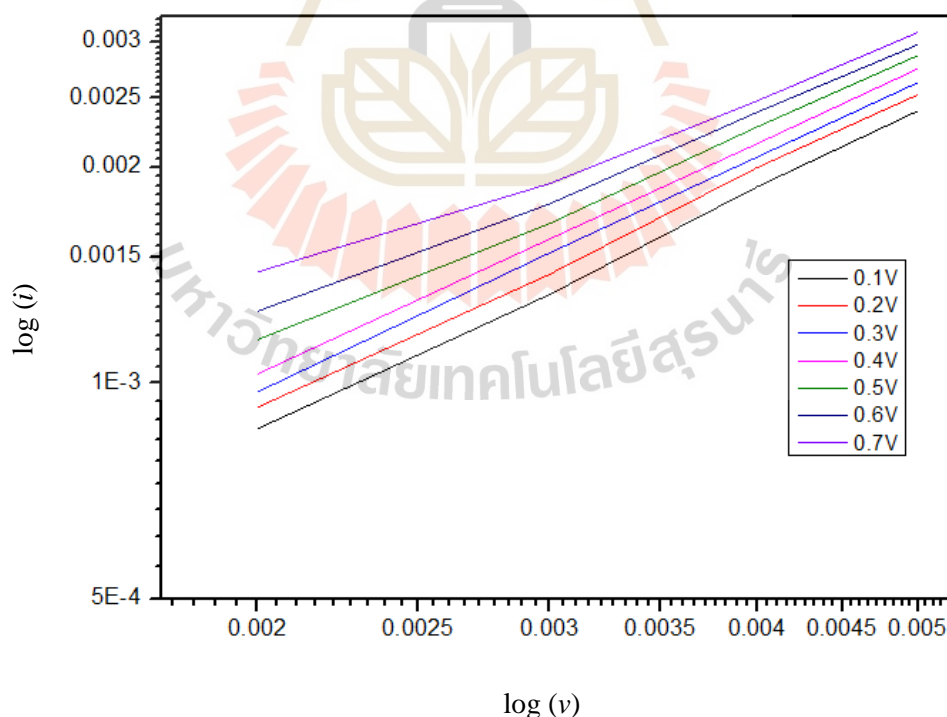


Figure 4.8 Plot of $\log(i)$ and $\log(v)$ used in b-value determining.

Among the surface contribution, the proportion of EDLC and redox-pseudocapacitance normally cannot be differentiated from each other because they both have the same response behavior to the scan rate. In this work, the mapping of CV profile obtained from varying electrolyte concentration is introduced as illustrated earlier. EDLC contribution is extracted from an overlapped rectangular area which represents the pure electrostatic capacitive characteristic. The remaining area corresponds to the contribution from pseudocapacitance. The EDLC and pseudocapacitance contribution on the total capacitance are distinguishable as shown in figure 4.9.

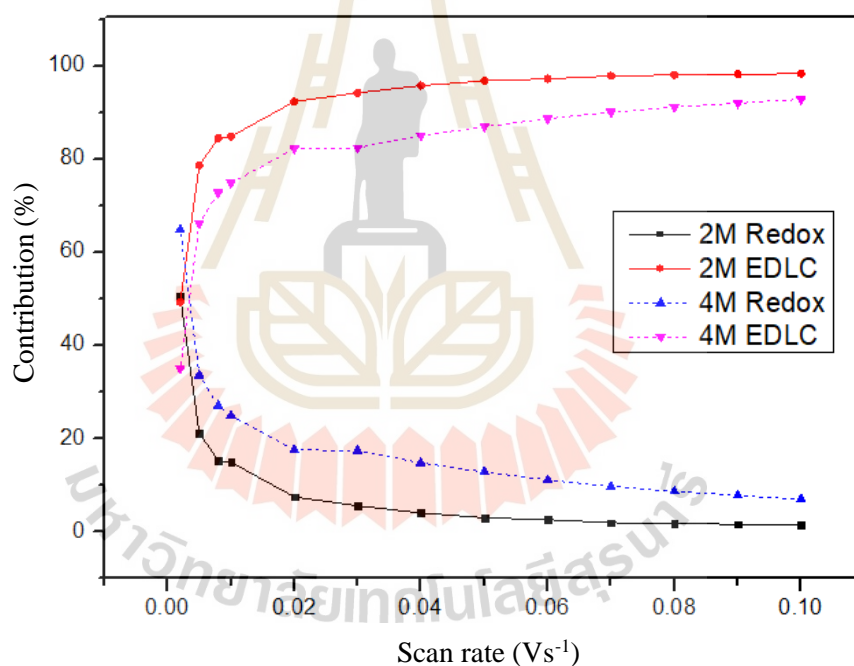


Figure 4.9 Contribution of EDLC and redox reaction on total specific capacitance of 2M and 4M electrolyte concentration.

On the average, the EDLC contribution is greater than pseudocapacitance as expected because all samples are carbon-based electrode which have high surface area but low chemical activity. Interestingly, at the scan rate of 2 mVs⁻¹, EDLC (50.6%) and pseudocapacitance (49.4%) share a nearly equal contribution in 2M condition while the

contribution from pseudocapacitance (64.9%) is even greater than EDLC (35.1%) in 4M condition. The pseudocapacitance contribution, in both cases, trends to decrease and almost vanish with the increase of scan rate. This implies the influence of charging rate on the chemical redox activity. On the other hand, EDLC contribution increase with the scan rate because the higher scan rate result in higher potential gradient and therefore higher electric field strength. Combination of both EDLC and pseudocapacitance results in an excellence rate capability with maximum capacitance peak. This also indicates a good mobility of ions in aqueous electrolyte and the intense electric field of planar electrode structure.

To provide further understanding of the apportion between EDLC and redox contribution among the total capacitance, the simplified model is proposed. Starting from the total charge electrolyte ions in the system, some of them are consumed in the chemical redox reaction process. The redox contribution is dominated at low scan rate and decrease exponentially because shorten of the allowable reaction time as illustrated in figure 4.10. The simplified mathematical model of this redox contribution is as the following

$$C_{Re}(v) = a_0 e^{-a_1 v} \quad (4.1)$$

where a_0 and a_1 are fitting parameters and v is scan rate

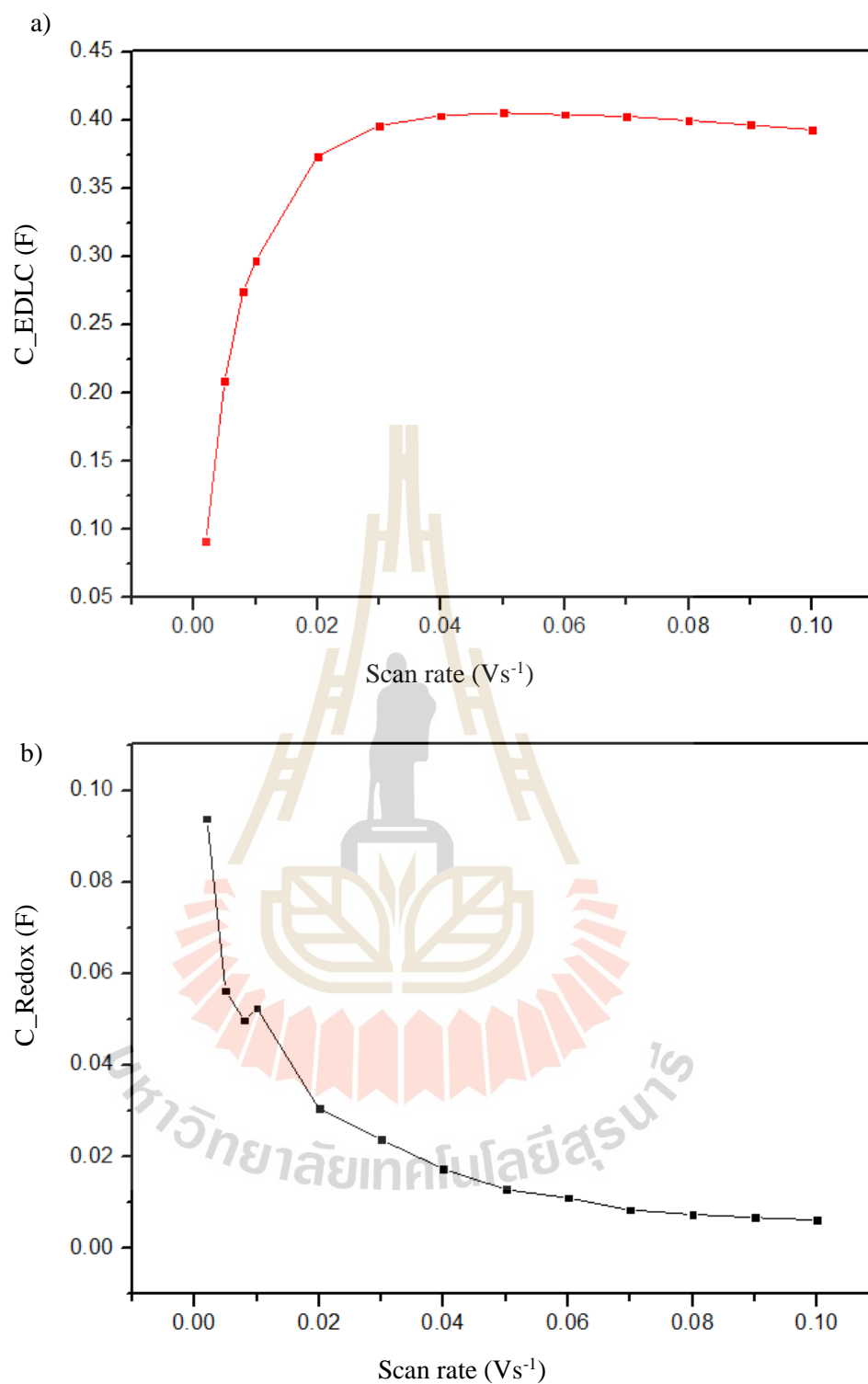


Figure 4.10 a) EDLC and b) redox contribution on the total capacitance.

Some of the remaining ions are consumed in the EDLC charging process. Since the redox contribution is relatively high at low scan rate, the amount of remaining ions for EDLC contribution is relatively low at the initial state. When the scan rate increase, the redox contribution decreases exponentially as explained above. Therefore, there are larger amount of the remaining ions resulting in the exponentially increase of EDLC contribution. Unavoidably, the internal resistance of the device and nature of electrolyte restrict the mobility of ions themselves. Some of the remaining ions may not be able to move and attach to the accessible electrode surface, the EDLC contribution is therefore deduced as the scan rate increase. The simplified mathematical model of this EDLC contribution is as the following

$$C_{EDLC}(v) = b_0(1 - b_1 e^{-b_2 v}) - b_3 v \quad (4.2)$$

where b_0 , b_1 , b_2 and b_3 are fitting parameters and v is scan rate.

The first term is an exponentially increase term and the second term is the deduction term. The later term may consider as the IR drop occurring in the galvanostatic charge/discharge (GCD) measurement. The proposed model is in good agreement with the experimental result and provides the reasonably physical meaning. The figure 4.11 shows the fitting results obtained from the simplified model. In order to verify the model, the plot of redox and EDLC contribution ratio obtained from both experimental measurement and proposed equation are presented in figure 4.12. The variance, goodness of fitting, is 0.935 which indicates the good agreement of the fit.

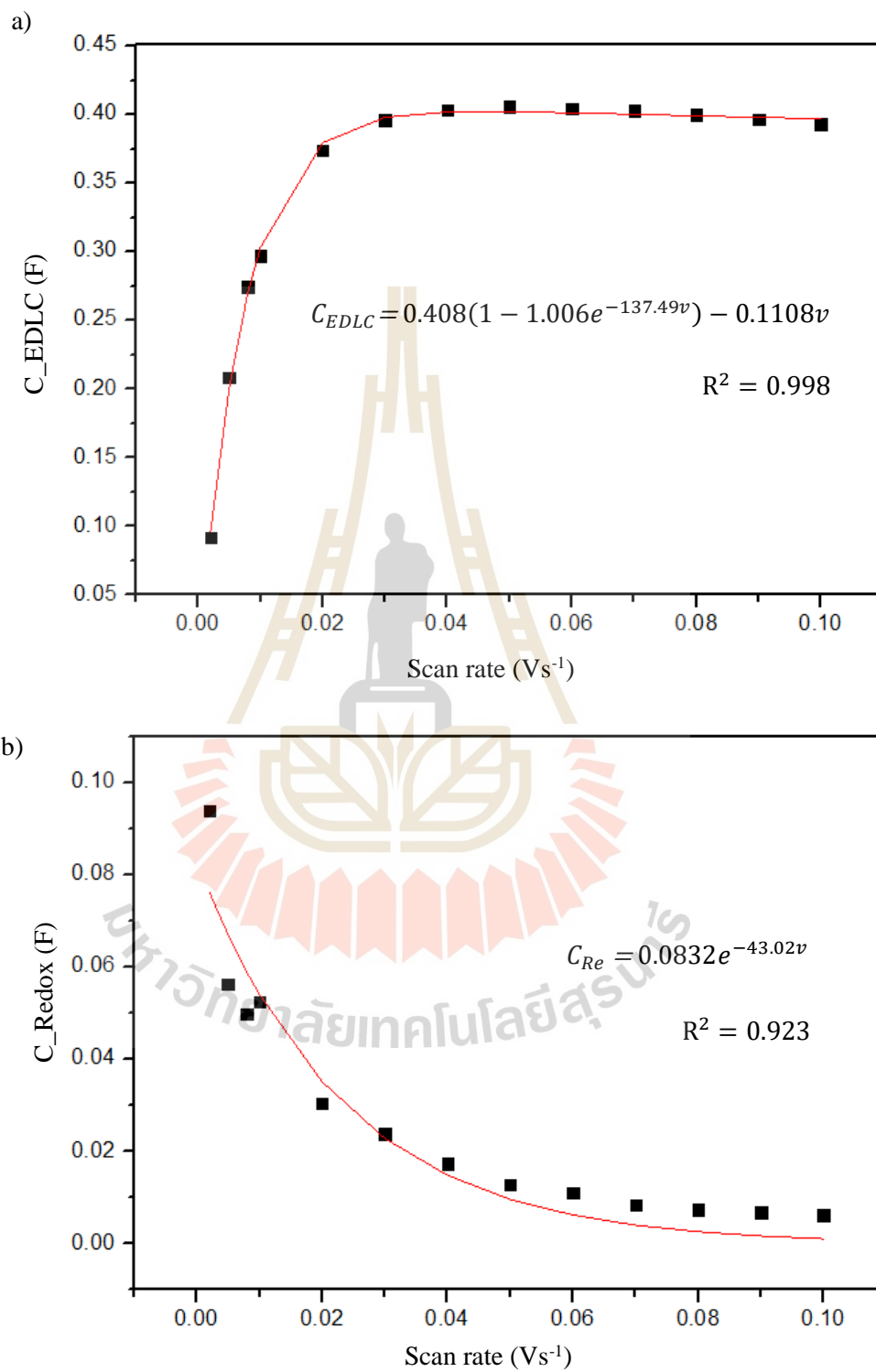


Figure 4.11 Simplified mathematical model fitting of a) EDLC and b) redox contribution.

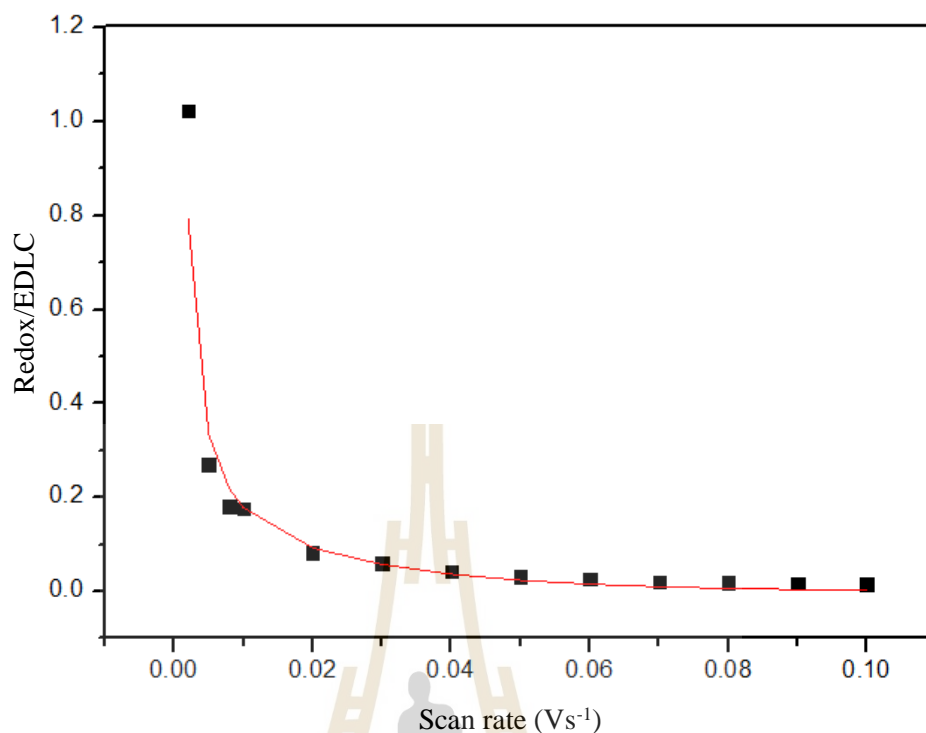


Figure 4.12 Ratio between redox and EDLC contribution.

4.2.3 Further discussion on the influence of electrode geometry on the cell capacitance

As the experimental and simulation results indicate the superior advantage of using planar electrode configuration in the aspect of larger specific capacitance and better rate capability beyond the conventional sandwich structure, the design of the electrode geometry is the crucial concern. The planar electrode with the narrow electrode fringe seems to provide the most excellent electrochemical performance. This narrow fringe design provides a very large amount of specific capacitance and be able to withstand the increase of the charging rate more than 100 times because of the short diffusion path and edge effect. With the corporate of the printing technology, one may attempt to fabricate the planar electrode which has a very thin electrode fringe and very small gap space. Too small and too closed electrode fringe may cause two problems.

First, the too small electrode fringe will lose the conductivity because the resistance of the current collector increase if the electrode is too small. The overall performance of the cell may be dropped down. Second, the electrodes that are placed too closed to each other may cause the circuit break down because of the voltage applied between the adjacent electrodes. Type of current collector, type of active material, type of electrolyte and also phase of electrolyte (solid state, gel or liquid) are need to be consider for the suitable design and selected of planar electrode geometry.



CHAPTER V

CONCLUSIONS

5.1 Conclusions

Carbon-based supercapacitor with comb-like planar electrodes were prepared. The width of electrode fringe was varied while the interspace between fringes were fixed. All samples were put in 3D printing case filled with an aqueous sodium nitrate electrolyte and the specific capacitance were investigated using cyclic voltammetry measurement. With the same amount of active material mass, planar electrode can provide higher specific capacitance than the conventional sandwich structure with the maximum 86.7% enhancement. Simulation result of electric field intensity according to the geometry of each electrode configuration has a good agreement with the specific capacitance observed. The narrower the electrode fringe, the higher electric field and higher specific capacitance. Unusual capacitance rate capability were observed in all planar samples. The specific capacitance was still higher than its initial value even the scan rate was increased 100 times. The CV profiles of planar electrode using difference electrolyte concentration were used to distinguish the contribution of EDLC and pseudocapacitance on the total value. Pseudocapacitance are dominated at low charging rate and converges to EDLC behavior at fast charging rate. The simplified mathematical model together with physical explanation of charge storage mechanism is proposed in order to serve as the initiation for further understanding and improvement. Beside the characteristic of active material, planar electrode structure provides an effective

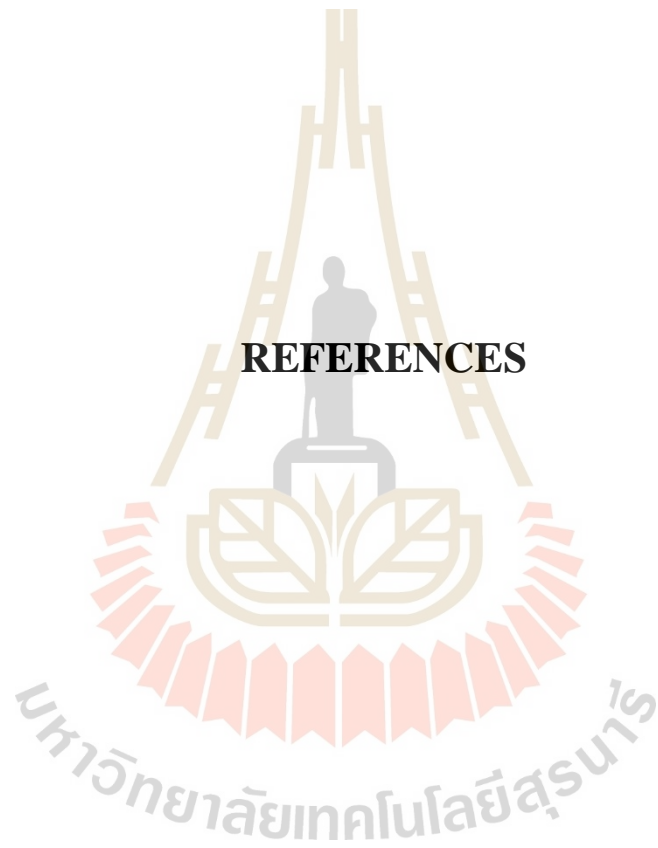
approach to increase the specific capacitance of supercapacitor at high charging rate due to its advantage on an intense electric field and facilitates good ions mobility beyond the conventional sandwich structure.

5.2 Future direction

This works aims to provide the alternative to enhance the performance of supercapacitor. Instead of focus only on the active material, the electrode arrangement is taking into account. The results show that planar electrode configuration play an important role on the charging characteristic and the total capacitance of the device.

The outstanding rate capability which indicates that there is an optimum charging rate for a particular electrode configuration may be used as the based idea to further develop the fast charging supercapacitor. Future work may attempt to determine the parameter which can control the optimum charging rate for any desire application. If successful, supercapacitor with high energy density and fast charging ability will benefit the energy storage device industry, especially in transportation section.

REFERENCES



REFERENCES

- Alanne, K., and Saari, A. (2006). Distributed energy generation and sustainable development. **Renewable and sustainable energy reviews**. 10(6): 539-558.
- Aneke, M., and Wang, M. (2016). Energy storage technologies and real life applications—A state of the art review. **Applied Energy**. 179: 350-377.
- Simon, P., Gogotsi, Y., and Dunn, B. (2014). Where do batteries end and supercapacitors begin?. **Science**. 343(6176): 1210-1211.
- Libich, J., Máca, J., Vondrák, J., Čech, O., and Sedlaříková, M. (2018). Supercapacitors: Properties and applications. **Journal of Energy Storage**. 17: 224-227.
- Jayalakshmi, M., and Balasubramanian, K. (2008). Simple capacitors to supercapacitors-an overview. **Int. J. Electrochem. Sci**. 3(11): 1196-1217.
- Iro, Z. S., Subramani, C., and Dash, S. S. (2016). A brief review on electrode materials for supercapacitor. **Int. J. Electrochem. Sci**. 11(12): 10628-10643.
- Chen, T., and Dai, L. (2014). Flexible supercapacitors based on carbon nanomaterials. **Journal of Materials Chemistry A**. 2(28): 10756-10775.
- Kondrat, S., Perez, C. R., Presser, V., Gogotsi, Y., and Kornyshev, A. A. (2012). Effect of pore size and its dispersity on the energy storage in nanoporous supercapacitors. **Energy & Environmental Science**. 5(4): 6474-6479.

- Baptista, J. M., Sagu, J. S., KG, U. W., and Lobato, K. (2019). State-of-the-art materials for high power and high energy supercapacitors: Performance metrics and obstacles for the transition from lab to industrial scale—A critical approach. **Chemical Engineering Journal**. 374: 1153-1179.
- Kim, C. H., Yang, C. M., Kim, Y. A., and Yang, K. S. (2019). Pore engineering of nanoporous carbon nanofibers toward enhanced supercapacitor performance. **Applied Surface Science**. 497: 143693.
- Simon, P., and Gogotsi, Y. (2008). Materials for electrochemical capacitors. **Nature materials**. 7(11): 845-854.
- Abdah, M. A. A. M., Azman, N. H. N., Kulandaivalu, S., and Sulaiman, Y. (2020). Review of the use of transition-metal-oxide and conducting polymer-based fibres for high-performance supercapacitors. **Materials & Design**. 186: 108199.
- Zhang, L., Yang, S., Chang, J., Zhao, D., Wang, J., Yang, C., and Cao, B. (2020). A review of redox electrolytes for supercapacitors. **Frontiers in Chemistry**. 8: 413.
- Fan, L. Z., and Maier, J. (2006). High-performance polypyrrole electrode materials for redox supercapacitors. **Electrochemistry communications**. 8(6): 937-940.
- Ryu, K. S., Kim, K. M., Park, N. G., Park, Y. J., and Chang, S. H. (2002). Symmetric redox supercapacitor with conducting polyaniline electrodes. **Journal of Power Sources**. 103(2): 305-309.

- Qi, D., Liu, Y., Liu, Z., Zhang, L., and Chen, X. (2017). Design of architectures and materials in in-plane micro-supercapacitors: current status and future challenges. **Advanced Materials**. 29(5): 1602802.
- Pech, D., Brunet, M., Dinh, T. M., Armstrong, K., Gaudet, J., and Guay, D. (2013). Influence of the configuration in planar interdigitated electrochemical micro-capacitors. **Journal of Power Sources**. 230: 230-235.
- Ghoniem, E., Mori, S., and Abdel-Moniem, A. (2016). Low-cost flexible supercapacitors based on laser reduced graphene oxide supported on polyethylene terephthalate substrate. **Journal of Power Sources**. 324: 272-281.
- Wu, Z. S., Parvez, K., Feng, X., and Müllen, K. (2014). Photolithographic fabrication of high-performance all-solid-state graphene-based planar micro-supercapacitors with different interdigital fingers. **Journal of Materials Chemistry A**. 2(22): 8288-8293.
- Khan, M., Rahaman, R., and Kang, S. W. (2015). Highly sensitive multi-channel IDC sensor array for low concentration taste detection. **Sensors**. 15(6): 13201-13221.

- Castiello, F. R., Porter, J., Modarres, P., and Tabrizian, M. (2019). Interfacial capacitance immunosensing using interdigitated electrodes: the effect of insulation/immobilization chemistry. **Physical Chemistry Chemical Physics**. 21(28): 15787-15797.
- Latimer, K. J., Evans, J. W., Cowell, M. A., and Wright, P. K. (2017). Modeling of interdigitated electrodes and supercapacitors with porous interdigitated electrodes. **Journal of The Electrochemical Society**. 164(4): A930.
- Olthuis, W., Streekstra, W., and Bergveld, P. (1995). Theoretical and experimental determination of cell constants of planar-interdigitated electrolyte conductivity sensors. **Sensors and Actuators B: Chemical**. 24(1-3): 252-256.
- Ratajczak, P. (2015). Design of high voltage AC/AC electrochemical capacitors in aqueous electrolytes.
- Shao, Y., Li, J., Li, Y., Wang, H., Zhang, Q., and Kaner, R. B. (2017). Flexible quasi-solid-state planar micro-supercapacitor based on cellular graphene films. **Materials Horizons**. 4(6): 1145-1150.

CURRICULUM VITAE

Name Mr. Ukrit Jitropas

Date of Birth February 25th, 1993

Place of Birth Nakhonratchasima, Thailand

E-mail u.jitropas@gmail.com

Education

2011-2015 B.Eng (Mechanical Engineering), Sirindhon International Institute of Technology, Thammasat University, Thailand

2015-2017 M.Sc. (Engineering and technology), Sirindhon International Institute of Technology, Thammasat University, Thailand

2018-present Ph.D. (Physics), Suranaree University of Technology, Thailand

Publications:

Jitropas, U., Yunphuttha, C., Siroroj, S., and Meevasana, W. (2020). Capacitance Optimization of Planar Carbon-based Supercapacitor. CHIANG MAI JOURNAL OF SCIENCE, 47(4): 607-613.

Jitropas, U., and Hsu, C. H. (2017). Study of the first-principles correlation functional in the calculation of silicon phonon dispersion curves. Japanese Journal of Applied Physics, 56(7): 070313.